Published in final edited form as:
J Comp Neurol. 2002 September 9; 451(1): 1–21.

Cell-Specific Expression of Plasma Membrane Calcium ATPase Isoforms in Retinal Neurons

David Krizaj[1,2,*], **Steven J. Demarco**[3], **Juliette Johnson**[2], **Emanuel E. Strehler**[3], and **David R. Copenhagen**[1,2]

1*Department of Physiology, University of California San Francisco, San Francisco, California 94143-0730*

2*Department of Ophthalmology, University of California San Francisco, San Francisco, California 94143-0730*

3*Department of Biochemistry and Molecular Biology, Mayo Clinic, Rochester, Minnesota 55905*

Abstract

Ca^{2+} extrusion by high-affinity plasma membrane calcium ATPases (PMCAs) is a principal mechanism for the clearance of Ca^{2+} from the cytosol. The PMCA family consists of four isoforms (PMCA1–4). Little is known about the selective expression of these isoforms in brain tissues or about the physiological function conferred upon neurons by any given isoform. We investigated the cellular and subcellular distribution of PMCA isoforms in a mammalian retina. Mouse photoreceptors, cone bipolar cells and horizontal cells, which respond to light with a graded polarization, express isoform 1 (PMCA1) of the PMCA family. PMCA2 is localized to rod bipolar cells, horizontal cells, amacrine cells, and ganglion cells, and PMCA3 is predominantly expressed in spiking neurons, including both amacrine and ganglion cells but is also found in horizontal cells. PMCA4 was found to be selectively expressed in both synaptic layers. Optical measurements of Ca^{2+} clearance showed that PMCAs mediate Ca^{2+} extrusion in both rod and cone bipolar cells. In addition, we found that rod bipolar cells, but not cone bipolar cells possess a prominent Na^+/Ca^{2+} exchange mechanism. We conclude that PMCA isoforms are selectively expressed in retinal neurons and that processes of Ca^{2+} clearance are different in rod and cone bipolar cells.

Indexing terms

PMCA; Ca^{2+} extrusion; photoreceptor; bipolar cell; Na/Ca exchange

Ca^{2+} functions as a critical and ubiquitous second messenger by regulating a variety of key intracellular processes (Berridge et al., 2000). The concentration of free intracellular Ca^{2+} ions, $[Ca^{2+}]_i$, is set by the balance between Ca^{2+} entry into the cytoplasm and Ca^{2+} removal by means of buffering proteins, uptake into intracellular organelles and extrusion across the plasma membrane. Together with Na^+/Ca^{2+} exchangers (NCXs), the plasma membrane calcium ATPases (PMCAs) are the principal mechanism for Ca^{2+} extrusion from most vertebrate cells.

The mammalian PMCA family is encoded by four genes whose protein products have been designated PMCA1–4 (reviewed in Guerini and Carafoli, 1998;Strehler and Zacharias, 2001). Expression studies in heterologous cell systems have revealed that the members of the family differ significantly in their affinities for Ca^{2+} and calmodulin and are linked differently

*Correspondence to: David Krizaj, Department of Ophthalmology, Beckman Vision Center, Room K-140, UCSF School of Medicine, 10 Kirkham Street, San Francisco, CA 94143-0730. E-mail: krizaj@phy.ucsf.edu
Dr. DeMarco's present address is Brain Research Institute, University of Zürich, CH-8057 Zürich, Switzerland.

to multiprotein complexes containing PDZ domain proteins (Enyedi et al., 1994;DeMarco and Strehler, 2001;Caride et al., 2001b). PMCA isoforms also are differentially regulated by intracellular messengers such as protein kinases A and C, proteases, and acidic phospholipids (reviewed by Monteith and Roufogalis, 1995;Penniston and Enyedi, 1998;Strehler and Zacharias, 2001). However, immunolocalization of PMCA isoforms to different neuron subtypes within a tissue has hitherto been seldom carried out (de Talamoni et al., 1993;Dumont et al., 2001). Moreover, the functional significance of differential localization of the PMCA isoforms to central nervous system (CNS) tissues and to different cell types is poorly understood.

The vertebrate retina consists of cell types with different light response properties. Some classes of retinal neurons signal with graded potentials (photoreceptors, horizontal and bipolar cells), others communicate by means of action potentials (ganglion cells), and still others use both graded and action potentials (amacrine cells; Werblin and Dowling, 1969;Kolb, 1995;Bieda and Copenhagen, 1999). Spiking induces transient elevations in $[Ca^{2+}]_i$ compared with the sustained elevations in nonspiking, graded potential neurons. Bipolar, amacrine, and ganglion cells can be further divided into ON and OFF subclasses, which respond to light with depolarization and hyperpolarization, respectively (Werblin and Dowling, 1969). These differences in light-evoked responses presumably place very different demands on the calcium regulation systems of different classes of retinal neuron. In this study, we examine the hypothesis that functionally highly diverse populations of retinal neuron rely on different Ca^{2+} extrusion mechanisms.

By using electrophysiological methods and optical imaging techniques, Ca^{2+} extrusion from photoreceptor terminals in tiger salamander and tree shrew was shown to be exclusively mediated by a PMCA-like mechanism (Krizaj and Copenhagen, 1998;Morgans et al., 1998). In contrast, a Na^+/K^+,Ca^{2+} exchanger mechanism mediates Ca^{2+} extrusion from photoreceptor outer segments, suggesting that Ca^{2+} clearance is highly compartmentalized in different regions of the same cell (Miller et al., 1994;Krizaj and Copenhagen, 1998). The localization of PMCAs to synaptic terminals of rods and cones was confirmed by immunohistochemistry by using a pan-specific PMCA antibody (Morgans et al., 1998;Krizaj and Copenhagen, 1998). However, it is not known which particular PMCA isoforms are expressed in photoreceptors.

The mechanisms of Ca^{2+} extrusion from bipolar cells are currently unclear. In one study, Ca^{2+} efflux from synaptic terminals of teleost bipolar cells was shown to be mediated exclusively by PMCA-like extrusion mechanisms (Zenisek and Matthews, 2000). However, Kobayashi and Tachibana (1995) found evidence for Na^+/Ca^{2+} exchanger-mediated Ca^{2+} extrusion from these same type of fish bipolar cells. No information is available about Ca^{2+} extrusion systems used in mammalian bipolar cells.

PMCA-mediated Ca^{2+} efflux also contributes to Ca^{2+} extrusion from third-order retinal neurons (Gleason et al., 1994,1995). In cultured chick amacrine cells, PMCAs contribute from ~0 to ~50% of total Ca^{2+} clearance (Gleason et al., 1995). A Na^+/Ca^{2+} exchange mechanism constitutes the remaining component of Ca^{2+} extrusion. Na^+/Ca^{2+} exchange also may be prominent in fish ganglion cells (Bindokas et al., 1994). However, no PMCA-dependent Ca^{2+} extrusion has yet been detected in retinal ganglion cells. From the above, it is clear that much still needs to be learned about Ca^{2+} extrusion mechanisms from neurons in the mammalian retina. Moreover, the PMCA isoforms associated with Ca^{2+} extrusion from specific retinal cell classes have yet to be identified.

The aim of the current study was to map and compare the distribution and cellular localization of all PMCA isoforms in a mammalian retina. Particular attention was paid to photoreceptors

and bipolar cells, cell types that are the most likely to rely on PMCA-mediated extrusion of Ca^{2+} (Kobayashi and Tachibana, 1995;Krizaj and Copenhagen, 1998;Zenisek and Matthews, 2000). We report here that PMCA isoforms are differentially distributed within different classes of retinal neuron and to different subcellular locations within neurons. Specifically, we found that photoreceptors and cone bipolar cells possess PMCA1, rod bipolar cells express PMCA2, whereas the spiking amacrine and ganglion cells express both PMCA2 and PMCA3. PMCA4 was present in synaptic structures of several retinal neurons. We propose that differential expression of PMCA isoforms in different classes of retinal neurons is likely of fundamental importance for the synaptic communication of the visual signal.

MATERIALS AND METHODS

Animals and tissue preparation

Retinas of adult C57BL/6 mice (Simonsen, Gilroy, CA) were investigated. All procedures were in accordance with National Institutes of Health guidelines and were approved by the Committee on Animal Research at University of California at San Francisco. The animals were anesthetized and killed with CO_2 asphyxiation followed by cervical dislocation. The eyes were enucleated, corneas were opened with a razor blade, and the eyecups with the retinas were immersion-fixed for 1.5 hours in 4% (w/v) paraformaldehyde in phosphate buffer (PB; 0.1 M; pH 7.4). The retinas were rinsed two times in PB and cryoprotected in 30% sucrose overnight at 4°C. Pieces of retinas were mounted in OCT, sectioned vertically at 14 μM thickness on a cryostat, and collected on Super-Frost Plus slides (Fisher, Pittsburgh, PA) and stored at −20° C until use.

Immunohistochemistry

The isoform-specific anti-PMCA antibodies were a generous gift from Adelaida Filoteo and John T. Penniston (Mayo Clinic, Rochester, MN). Rabbit polyclonal antibodies NR1, NR2, and NR3 against PMCA1, 2, and 3, respectively, were generated against 13-18 residue peptide sequences at the amino terminus of the corresponding rat PMCA (Filoteo et al., 1997). Mouse monoclonal antibody JA9/NR4 was raised against human erythrocyte PMCA and recognizes a sequence close to the N-terminus of PMCA4 (Caride et al., 1996). The specificity of all antibodies has been fully characterized by Western blots of COS cell microsomes containing overexpressed PMCAs of known identity (Filoteo et al., 1997). These antibodies have been used previously for immunostaining (Dumont et al., 2001).

The retinal sections were washed in PB for 15 minutes, then permeabilized and blocked in a solution containing 0.5% Triton X-100 and 10% goat serum. The antibody dilutions were 1:300–1:1,000 for PMCA1; 1:300–1:1,000 for PMCA2, 1:300–1:600 for PMCA3, and 1:100–1:500 for PMCA4. For double-labeling experiments, a mixture of primary antibodies was applied. Monoclonal antibodies against several classes of protein markers for retinal cells were co-applied with a polyclonal antiserum against one of the PMCA isoforms. These antibodies included those reactive for protein kinase C (PKC) (α, β, and γ isoforms; clone MC5, Santa Cruz Biotechnology, Santa Cruz, CA; used at 1:100 dilution); glutamic acid decarboxylase 65 (GAD-65; 1:500); SV2 (K. Buckley; Developmental Studies Hybridoma Bank, University of Iowa; 1:100); PSD-95 (Affinity BioReagents clone 7E3-1B8, Golden, CO; 1:200); calbindin D-28K (Sigma, St Louis, MO; 1:200), choline acetyltransferase (Chemicon MAB305; 1:50 to 1:300); vesicular glutamate transporter (VGLUT1, polyclonal rabbit; 1:3,000; a gift from Dr. Robert Edwards from UCSF), and β-galactosidase (1:50; Chemicon MAB1802).

We used the following secondary antibodies: Alexa 488 and Alexa 594 nm goat anti-mouse or goat anti-rabbit immunoglobulin G (H+L) conjugates (Molecular Probes, Eugene, OR), diluted at 1:1,000. After incubation, sections were washed in PB and mounted with Vectashield

(Vector, Burlingame, CA). Negative controls were performed for every set of experiments by omitting the primary antibody.

Immunoblotting

Western blot analysis of PMCA isoform expression in the adult mouse retina was performed essentially as described previously by Usachev et al. (2001). Briefly, two retinae (stored frozen at −70°C) were placed in a 1.5-ml test tube, and 200 μl of 2× Laemmli buffer (Ausubel et al., 1998) without bromophenol dye and DTT, but containing a protease inhibitor cocktail and 4 mM EDTA were added. The samples were resuspended, heated at 95°C for 3 minutes, sonicated briefly (3 × 1 second at 20% power output) to reduce the viscosity, and centrifuged for 10 minutes at 13,000 g. The protein concentration in the supernatant was determined by the BCA assay (Pierce, Rockford, IL). After adding 2× Laemmli buffer containing dye and 100 mM DTT, 40 μg of total protein lysate per lane were separated on 7.5% sodium dodecyl sulfate (SDS) -polyacrylamide gels, blotted onto polyvinylidene difluoride (PVDF) membrane, and processed for Western blotting by using PMCA isoform-specific antibodies as described (Usachev et al., 2001).

Ca^{2+} imaging

Ca^{2+} imaging of isolated mouse bipolar cells was performed as described (Krizaj et al., 1999;Akopian et al., 2000). In brief, single bipolar cells were dissociated by using papain (Akopian et al., 2000). After washing with Ringer's solution (composition [in mM]: NaCl 115, KCl 5.0, $MgCl_2$ 1.0, $CaCl_2$ 1.8, HEPES 5.0, glucose 5.0, pH 7.4), cells were triturated in L-15 medium (Life Technologies, Grand Island, NY) supplemented with (in mM) glucose 5.0, HEPES 9.5, and 1 mg/ml bovine serum albumin, and then plated onto sterilized glass coverslips coated with poly-lysine (0.1 mg/ml). Cells were loaded with the calcium indicator dye fura-2 AM (2–5 μM, Molecular Probes). After loading and washout of fura-2 AM, cells were depolarized with high K^+ solutions in which K^+ replaced equimolar amounts of Na^+. In Na^+-free solutions $[Na^+]_o$ was substituted by equimolar amounts of $[Li^+]_o$. The dye was excited periodically with 340/380-nm beams controlled by a Lambda-10 shutter/filter wheel controller (Sutter Instruments, Novato, CA) and Metafluor 4.1 software (Universal Imaging Corp., West Chester, PA). The background noise was corrected for by subtracting from each pair of images two "background" images acquired from the same coverslip in the absence of cells. In some experiments, the dissociated cells were fixed for 15 minutes in 4% (w/v) paraformaldehyde in phosphate buffer saline (PBS; 0.1 M; pH 7.4, room temperature) and processed for immunocytochemistry.

Image acquisition and processing

Immunofluorescent and bright-field Nomarski fields of view were obtained by using a confocal microscope (Bio-Rad MRC 1024 or Zeiss LSM 5 Pascal) at 10% power for the 488-nm argon line and 100% power for the 594 nm line. During acquisition of signals from double-labeled sections, the scans were collected sequentially to prevent spectral bleed through. Acquired images were processed with Adobe Photoshop (version 5.5) software.

RESULTS

All four PMCA isoforms are expressed in the mammalian retina

We used isoform-specific antibodies for Western blotting to determine which principal PMCA isoforms are expressed in the mouse retina. Total mouse retina proteins were separated by SDS-polyacrylamide gel electrophoresis, transferred to PVDF membranes, and incubated with affinity-purified antibodies (NR1, NR2, NR3, and JA9; Filoteo et al., 1997). 5F10, a high affinity monoclonal antibody known to recognize all PMCA isoforms was used as a control

(de Talamoni et al., 1993;Filoteo et al., 1997). 5F10 has already been shown to immunoreact with the amphibian and mammalian retina (Krizaj and Copenhagen, 1998;Morgans et al., 1998). The results of the Western blot analyses are summarized in Figure 1 and show that all four major isoforms are present in the mouse retina. We next used immunohistochemistry to determine the distribution of PMCA isoforms among specific retinal cell types.

PMCA1 is expressed in photoreceptors and bipolar cells

Confocal fluorescent images of transverse sections of mouse retina immunostained with antibodies against PMCA1 showed that this isoform is prominently expressed in the outer plexiform layer (OPL). Less intense staining was observed in the inner plexiform layer (IPL) and inner nuclear layer (INL) (Fig. 2A). In the INL, cell somata and radial processes of bipolar cells were both stained by the PMCA1 antibody. The antibodies also diffusely immunolabeled the IPL with a concentration of immunoreactivity in two prominent lateral strata.

In the OPL, PMCA1 expression was much more prominent presynaptically, i.e., in photoreceptor synaptic terminals, than postsynaptically, i.e., in dendrites of horizontal and bipolar cells. Retinal sections were double-immunolabeled with antibodies to PMCA1 and to SV2, an abundant Ca^{2+}-dependent synaptic vesicle protein that is expressed in photoreceptor terminals (Vu et al., 2000). Figure 3A,B shows the PMCA1 and SV2 signals, respectively, in the OPL (Fig. 3B). Figure 3C shows the two images combined. PMCA1 colocalized with SV2, proving that this PMCA isoform is expressed in photoreceptor synaptic terminals. PMCA1 was also prominently expressed in the inner segments of photoreceptors, distal to synaptic terminals (Fig. 3A). Similar colocalization of PMCA1 and another synaptic terminal marker, PSD-95 (Koulen et al., 1998;Vu et al., 2000) was also found (data not shown). PMCA1 was abundantly expressed in rod spherules, which have diameters of 1–2 μm and line the distal margin of the OPL. Because cones are only a small fraction of the photoreceptors in the mouse retina (Szel et al. 1996;Koulen et al., 1998), we could not demonstrate unequivocal staining in cone terminals by PMCA1 antibody. However, when we immunostained macaque monkey and tiger salamander retinae with PMCA1 antibodies, it was clear that cone pedicles also express PMCA1. Figure 3J–L demonstrates, that PMCA1 is expressed in both rod and cone photoreceptor terminals in the retina of the monkey. Note the remarkably uniform labeling of synaptic terminals of both rod spherules and cone pedicles in the monkey retina, which suggests that PMCA1 is expressed across the whole surface of the terminal. Similar results were observed in the salamander retina (D.K. and D.R.C., manuscript in preparation). On this basis, we surmise that PMCA1 was very likely expressed in cone terminals of mouse.

To investigate the level of PMCA1 expression in horizontal cells, we immunolabeled retinal sections for calbindin, a known marker of rodent horizontal cells (Pasteels et al., 1990). We find weak expression in the horizontal cell processes compared with photoreceptors. Figure 3D–I is a view at high magnification of the mouse OPL, stained for PMCA1 and calbindin. As reported previously, calbindin-immunopositive cells in the mouse retina include horizontal cells as well as populations of amacrine and ganglion cells (Pasteels et al., 1990;Haverkamp and Wässle, 2000). Calbindin-immunostained horizontal cells are characterized by a large soma ramifying throughout the distal edge of the inner nuclear layer and by dendrites that enter the photoreceptor terminals (Fig. 3E; small arrowheads) and end as small swellings within the synaptic terminals of photoreceptors (shown labeled by the anti-PMCA1 antibody in Figs. 3A,D,G, 4A,D). At higher magnification (Fig. 3G–I), each calbindin-positive knob is ringed by a PMCA1-labeled terminal (Fig. 3I). These data emphasize the preponderance of PMCA1 expression in the rods and cones. However, our data also reveal that, in the OPL, the PMCA1 epitope is weakly expressed in horizontal cell bodies and processes (arrowhead in Fig. 3D). Moreover, in the INL, a moderate staining of cell bodies of several bipolar cells was observed. In contrast to the weak immunoreactivity of the calbindin-positive horizontal cells, we could

detect no PMCA1 immunoreactivity in third-order calbindin expressing neurons located in the INL and GCL. These results are described below.

PMCA1 is expressed in cone but not rod bipolar cells—The immunostaining pattern observed in the INL suggested PMCA1 localization to bipolar cells (Fig. 2). PMCA1 was expressed in the ellipsoid-shaped cell bodies localized in the INL proximal to horizontal cells (Fig. 3A,D). In addition, significant immunoreactivity for PMCA1 was observed in the IPL (Fig. 2). Given that PMCA1 stained bipolar cell-like somata, but was excluded from calbindin-immunopositive amacrine cells, we focused on its possible presence within bipolar cells. The location of bipolar synaptic terminals in the IPL is often used as a selective marker for categorization of bipolar cells into ON and OFF response types, respectively (Famiglietti et al., 1977). The inner plexiform layer can be divided into the distal region (sublamina a) closer to the INL, where synaptic interactions of the OFF retinal pathway occur, and a proximal region (sublamina b), near the ganglion cell layer, where synaptic processes of ON cells reside (Famiglietti et al., 1977). Several classes of ON bipolar cells have been identified in the rodent retina, including four types of cone bipolar cells and an abundant class of rod bipolar cells (Euler and Wässle, 1995;Haverkamp and Wässle, 2000). As seen in Figure 4A,C, PMCA1 immunolabeling was concentrated both in the sublamina a of the IPL where the terminals from OFF bipolar cells reside, as well as in the distal layer of sublamina b. This pattern of immunostained bipolar cell terminals corresponds to strata which are formed by the class 3 and 5 bipolar cells of the rat retina (Euler and Wässle, 1995). To determine whether rod (ON) bipolar cells expressed the PMCA1 antigen, we costained PMCA1-labeled retinas with an antiserum against PKC, a selective marker for rod bipolar cells (Negishi et al., 1988;Greferath et al., 1990). As predicted, PKC labeled a population of bipolar cells with synaptic terminals localized to the proximal layer of sub-lamina b (“ON lamina”) of the IPL (Fig. 4B). The PKC antibody did not label either PMCA1-immunopositive perikarya in the INL or synaptic terminals in the IPL (Fig. 4C), indicating that rod bipolar cells do not express PMCA1.

Using another cell-specific marker reveals that PMCA1 is expressed by the cone ON bipolar cells. For these studies, we made use of retinal sections from transgenic mice in which the mGluR6 receptor gene was fused to a β-galactosidase (lacZ) reporter gene (Ueda et al., 1997). The metabotropic glutamate receptor mGluR6 controls the light responsive signaling cascade in both rod bipolar cells and ON cone bipolar cells (Masu et al., 1995;Ueda et al., 1997). The retinas were colabeled with antibodies against the lacZ antigen and PMCA1. We observed that the IPL in transgenic mice was generally labeled more prominently with the PMCA1 antibody compared with wild-type controls (e.g., compare Fig. 4A with D), but these differences were not further examined. The lacZ antibody stained a large population of bipolar cells comprising both rod and cone ON bipolar cells (Fig. 4E,F;Ueda et al., 1997). The perikarya of many lacZ-positive cells were also immunopositive for PMCA1 (Fig. 4F), strongly suggesting that this isoform is expressed in ON cone bipolar cells. In addition, the cell bodies of several lacZ immunonegative cells in the INL were stained with PMCA1 (arrow). We interpret this finding as suggestive of immunolocalization of PMCA1 to cone OFF bipolar cells. Many of the lacZ-immunopositive synaptic terminals in the sublamina b were immunoreactive to PMCA1 antibody. However, many of the larger-sized structures in the proximal part of sublamina b were not PMCA1 immunopositive (Fig. 4F; arrowheads). Taken together these results strongly suggest that PMCA1 is expressed in cone ON and OFF bipolar cells, but not in rod bipolar cells.

To further confirm the expression of PMCA1 in glutamatergic bipolar cell terminals we double-labeled retinas with PMCA1 and VGLUT1 antibodies. VGLUT1 is a vesicular glutamate transporter (Bellocchio et al., 1998) found in retinal glutamatergic neurons (Johnson et al., 2001). Unfortunately, VGLUT1 antibody is a rabbit polyclonal just like the PMCA antibodies used in this study, precluding a direct colocalization study of these two proteins. To determine

whether the PMCA1 immunolabeling in the IPL corresponds to the labeling of neurons with glutamatergic terminals (i.e., bipolar cells), we colabeled serial sections of the mouse retina with combinations of PMCA1/ PKC and VGLUT1/PKC antisera. Anti-VGLUT1 antibody strongly labeled the OPL (not shown, Johnson et al., 2001) as well as the IPL in the mouse retina. Three distinct VGLUT1-immunopositive signals were observed in the IPL: (1) large globular structures in the proximal region of sublamina b which costained with PKC (Fig. 4H,I). These were taken as an indication of the glutama-tergic terminals of rod bipolar cells). (2) Smaller puncta inserted just distal to the terminals of rod bipolar cells, presumably belonging to cone ON bipolar cells, and (3) small boutons located in sublamina a, which we take to be indicators of synaptic terminals of OFF bipolar cells (Fig. 4G–I). The VGLUT1-positive structures in the proximal half of sublamina b were not labeled with PMCA1 (Fig. 4A–I), supporting our hypothesis that PMCA1 is not expressed by rod bipolar cells. The smaller puncta, localized in sublamina a above the PKC-immunopositive layer, were labeled by both VGLUT1 and PMCA1. These data are suggestive of the expression of PMCA1 in synaptic terminals of cone ON and OFF bipolar cells. Taken together with the observation that the perikarya of cone bipolar cells, but not amacrine cells (see below), express PMCA1, we conclude that the majority of the PMCA1 signal in the IPL belongs to cone bipolar cells.

Na^+/Ca^{2+} exchange is evident in rod but not cone bipolar terminals

The finding that PMCA1 is expressed in cone but not rod bipolar cells raises the interesting issue of possible differences in Ca^{2+} regulation between these two classes of cell. Kobayashi and Tachibana (1995) found that Ca^{2+} extrusion from the mixed rod/cone Mb1 bipolar cells of teleost fish retina encompassed both Na^+/Ca^{2+} exchange and Ca^{2+} pumping by means of PMCAs. To determine whether Na^+/Ca^{2+} exchange plays a role in Ca^{2+} extrusion from mammalian bipolar cells, we performed Ca^{2+} imaging during and after depolarization-evoked responses from synaptic terminals of presumed rod and cone bipolar cells. Rod and cone bipolar cells were distinguished on the basis of their morphology and PKC immunoreactivity. As observed previously in rat (Pan, 2000), we found a major population (>90%) of bipolar cells isolated from the mouse retina was immunopositive for PKC. These cells correspond to the well-characterized class of rod bipolar cells and were easily identified by several unique morphologic features including the shape of their dendritic trees, the bushy soma and a single large synaptic terminal (Fig. 5B; see also Greferath et al., 1990;Haverkamp and Wässle, 2000;Pan, 2000). Figure 5A illustrates the $[Ca^{2+}]_i$ signal from a synaptic terminal of such a rod bipolar neuron loaded with the calcium indicator dye fura-2.

$[Ca^{2+}]_i$ in the synaptic terminal of this cell was elevated by high K^+-mediated depolarization. When the cell was subsequently exposed to low K^+ saline in which Na^+ was replaced by Li^+, the recovery rate of $[Ca^{2+}]_i$ in the terminal was significantly prolonged in comparison to control exposures to Na^+-containing saline (Fig. 5B). In 4/4 cells, the time constants of recovery were prolonged from 67 ± 20 seconds for the controls to 329 ± 137 seconds for the cells depolarized in the absence of $[Na^+]_o$. Similar results were observed in cell bodies of rod bipolar cells in which the recovery time constants increased from 58 ± 12 seconds for controls to 197 ± 69 seconds in the absence of $[Na^+]_o$. We have shown previously that Li^+ substitution selectively blocks Na^+/Ca^{2+} exchange but has little effect on PMCA-mediated Ca^{2+} extrusion (Krizaj and Copenhagen, 1998). This result, therefore, demonstrates that Na^+/Ca^{2+} exchangers play an important role in Ca^{2+} clearance from rod bipolar cells in the mammalian retina. The finding that Li^+ substitution merely slowed the rate by which $[Ca^{2+}]_i$ fell after elevation, is consistent with the idea that PMCA-mediated extrusion also functions here. Below, we present evidence that rod bipolar cell terminals express the PMCA2 isoform.

We also examined Ca^{2+} regulation in another class of bipolar cells that constituted a smaller (~5%) proportion of dissociated bipolar cells. These cells typically had smaller synaptic

terminals and sparser dendritic trees than did rod bipolar cells and did not immunoreact with the PKC antibody (Fig. 5C). Based on these features, we classified these cells as putative cone bipolar cells (Euler and Wässle, 1995;Pan, 2000). Because it was not possible to reliably record $[Ca^{2+}]_i$ changes from synaptic terminals of these cells due to their fragility and small size, all our data were derived from the cell bodies. As in rod bipolar cells, high K^+ was an effective stimulus for raising $[Ca^{2+}]_i$. However, as shown in Figure 5D, Li^+ substitution had no effect on the rate of Ca^{2+} clearance. The recovery of $[Ca^{2+}]_i$ in cone bipolar cells was fit by two exponentials. The first time constant for $[Ca^{2+}]_i$ recovery in controls was 40 ± 7 seconds and, in the absence of $[Na^+]_o$ was 36 ± 7 seconds, not significantly different from controls (n = 4). These results strongly suggest that PMCAs, but not Na^+/Ca^{2+} exchangers, support Ca^{2+} extrusion from cone bipolar cells. We conclude that rod and cone bipolar cells differ with respect to their Ca^{2+} extrusion mechanisms.

PMCA1 is not expressed in third-order retinal neurons

We investigated whether PMCA1 is localized to amacrine cells by colabeling retinas with PMCA1 and amacrine cell selective antibodies. We examined GABAergic amacrine cells, which have a crucial role in shaping the receptive fields and temporal responsiveness of bipolar, amacrine, and ganglion cells and may constitute more than half of all amacrine cells in the mammalian retina. Certain subtypes of GABAergic cells provide negative feedback to bipolar terminals by means of conventional inhibitory synapses (Fletcher et al., 1998). To label the GABAergic cell population in mouse retina, we used an antibody against the GABA synthesizing enzyme GAD-65, which is localized to perikarya and terminals of GABAergic cells. In agreement with previous findings (Haverkamp and Wässle, 2000), the antibody labeled two rows of cell bodies localized at the inner margin of the INL (Figs. 6, 9) as well as three distinct strata in the IPL.

As illustrated in Figure 6, the perikarya of GAD-65–positive cells were not immunostained by PMCAl (arrowheads). Although PMCA1 was not expressed in the perikarya of GABAergic neurons in the INL, it was not possible to ascertain definitively that PMCA1 was also absent from their dendritic trees in the IPL.

We also found that PMCA1 did not colocalize with calbindin-immunopositive amacrine cells. Similar to previous studies (Pasteels et al., 1990;Haverkamp and Wässle, 2000), we found that the anti-calbindin antibody labeled certain perikarya at the INL/IPL border and other perikarya in the GCL (Fig. 3E, arrow). Among the most prominent calbindin-immunopositive cell types are the cholinergic amacrine cells within the INL and displaced amacrine cells in the GCL (Haverkamp and Wässle, 2000). These cells were never immunopositive for PMCA1.

In summary, these results demonstrate that PMCA1 is strongly expressed in photoreceptors, may be present at moderate levels in horizontal cells and is excluded from amacrine cell bodies. In the INL and the IPL of the mouse retina, PMCA1 is mainly localized to cone bipolar cells but is excluded from third-order neurons.

PMCA3 is preferentially expressed in third-order retinal neurons

PMCA3 is a relatively rare isoform found only in a small subset of CNS tissues such as the choroid plexus, cerebellar granule cells, and habenula (Stahl et al., 1992;Eakin et al., 1995;Stauffer and Guerini, 1995;Filoteo et al., 1997). Thus, we were surprised to find a pronounced PMCA3 signal in the mouse retina (Figs. 1, 7A). PMCA3 immunofluorescence was particularly intense in the inner retina (Fig. 7) and in the optic nerve layer.

In addition to its strong labeling of the IPL and the GCL, a more moderate signal was observed in the OPL. To test whether the OPL signal reflects immunolabeling of photoreceptor synaptic

terminals, we double-labeled retinas with PMCA3 and the presynaptic markers SV2 or PSD-95. PMCA3 was excluded from SV2- and PSD-95–immunopositive photoreceptor terminals (not shown). Moderate PMCA3 staining was detected in the OPL just below the photoreceptor terminal stratum. Although the PMCA3 signal colocalized with calbindin-immunopositive horizontal cells (Figs. 7, 8), we have not been able to determine conclusively whether PMCA3 expression is restricted to dendrites and cell bodies of horizontal cells and/or processes of Müller cells, which ramify in the OPL (Fig. 8A–F).

The PMCA3 antibody labeled retinal ganglion cell bodies as well as the cell bodies of displaced calbindin-immunopositive amacrine cells in the ganglion cell layer and those of other amacrine cells, located near the inner edges of the IPL (Pasteels et al., 1990). To determine whether PMCA3 is also expressed by GABAergic amacrine cells, we colabeled retinas with GAD-65.

Some, but not all, GAD-65–immunopositive cell bodies in the INL were also immunopositive for PMCA3 (Fig. 9D,E, arrowheads), suggesting that a significant subset of the GABAergic amacrine population expresses the PMCA3 isoform. Moreover, a higher magnification view of the IPL revealed colocalization of PMCA3- and GAD-65–immunopositive puncta, suggesting that this isoform is expressed in the dendritic trees of GABAergic amacrine cells (Fig. 9G–I). PMCA3 is localized to other amacrine cell classes as well. It is noteworthy that PMCA3 is expressed in the calbindin-immunopositive amacrine cell somata (Fig. 8F) in the IPL as well as in the displaced amacrine cells in the GCL (Fig. 8A,C). Many calbindin-immunopositive cells belong to one of the cholinergic amacrine cell types (Pasteels et al., 1990). In agreement with this observation, we also found that cell bodies of cholinergic ChAT (choline acetyltransferase) -positive cells also expressed PMCA3 (data not shown).

To determine whether PMCA3 was expressed by rod bipolar cells, double-labeling experiments were performed by using PKC as the marker for rod bipolar cells. No PMCA3 signal was detected in the cell bodies of rod bipolar cells in the INL, nor in bipolar dendrites in the OPL (Fig. 10A). To ascertain whether PMCA3 is localized to the synaptic terminals of rod bipolar cells, we acquired high-resolution confocal images of the sublamina b. The results are shown in Figure 10B1–3. PMCA3 was expressed in a high density punctate manner throughout the IPL (Fig. 10B2). These puncta likely represent small immunoreactive particles clustered in dendritic tips of amacrine cells and ganglion cells (Figs. 7-9). A comparison with the immunostaining pattern for the PKC-immunoreactive terminals of rod bipolar cells (Fig. 10B3) revealed little colocalization between PMCA3 and PKC.

We interpret the absence of colocalization in Figure 10B as evidence that PMCA3 is not expressed in synaptic terminals of rod bipolar cells. Thus, it is unlikely that PMCA3 is the isoform responsible for the PMCA-mediated Ca^{2+} extrusion from synaptic terminals of rod bipolar cells that we observed with Ca^{2+} imaging (Fig. 5A). We conclude that PMCA3 is predominantly localized to the plasma membrane of third-order neurons in the mouse retina.

PMCA2 is mostly concentrated within to the inner retina

PMCA2 expression is especially prominent in the brain (Hilfiker et al., 1994;Stauffer et al., 1995). This isoform has the highest affinity for calmodulin of all four isoforms and, thus, is able to confer to cells a higher sensitivity to low Ca^{2+} concentrations (Hilfiker et al., 1994;Strehler and Zacharias, 2001). PMCA2 is also expressed prominently in the mouse retina (Fig. 11).

PMCA2 signal in the mouse OPL was moderate and confined to the OPL sublayer where typically bodies and dendrites of horizontal cells reside, as evidenced by immunostaining with the calbindin antibody (Fig. 12A–C). In the IPL, PMCA2 colocalized with PKC-immunopositive synaptic terminals in the proximal region of sublamina b corresponding to

rod bipolar cells (Fig. 12D–I), suggesting that PMCA2 mediates Ca^{2+} extrusion from rod bipolar cell terminals. This immunolocalization pattern is consistent with the physiologically determined PMCA-mediated component of Ca^{2+} extrusion (Fig. 5B).

Amacrine cells in the INL and perikarya of cells in the GCL also were strongly stained by the PMCA2 antibody. As shown in Figures 11 and 12, PMCA2 immunoreactivity is heavily concentrated in two bands of the mouse IPL. Both bands were also stained with the antibody against choline acetyltransferase (ChAT), a marker for cholinergic amacrine cells (data not shown), suggesting that the PMCA2 is found within this class of amacrine cells. PMCA2 was also expressed in calbindin-immunopositive amacrine cells (not shown).

PMCA4

PMCA4 is considered a "housekeeping isoform" of Ca^{2+}-ATPases and is expressed in many classes of neuron (Stauffer et al., 1997). When mouse retinas were immunolabeled with the PMCA4-specific antibody JA9/NR4, it strongly labeled both plexiform layers of the retina (Fig. 13).

To determine whether PMCA4 is localized within synaptic terminals of retinal cells, we colabeled the retinas with anti-SV2. As shown in Figure 14A–C, colocalization of PMCA4 and SV2 signals was very pronounced, strongly suggesting that PMCA4 is expressed in synaptic terminals of photoreceptors as well as in synaptic processes of inner retinal neurons.

A magnified view of the OPL is shown in Figure 14D–F. PMCA4 and SV2 labels showed a remarkable degree of colocalization, suggesting that PMCA4 is involved in Ca^{2+} extrusion from photoreceptor synaptic terminals. A detailed analysis of the subcellular localization of PMCA4 will not be considered here and will appear as part of a subsequent publication (D.K. and D.R.C., manuscript in preparation).

DISCUSSION

Our results show that all four PMCA isoforms are expressed in the mouse retina. Figure 15 summarizes the distribution of the four PMCAs in different neuronal cell types of the retina.

Our data extend earlier functional studies that showed that Ca^{2+} extrusion by means of PMCAs plays an impor-tant role in $[Ca^{2+}]_i$ regulation in several classes of retinal neurons, including photoreceptors, bipolar cells, horizontal cells, and amacrine cells (Gleason et al., 1995;Kobayashi and Tachibana, 1995;Krizaj and Copenhagen, 1998;Micci and Christensen, 1998;Morgans et al., 1998;Zenisek and Matthews, 2000). Our findings indicate that Ca^{2+} extrusion mechanisms in photoreceptors and bipolar cells, which respond to light by means of graded sustained potentials, differ from those found in spiking amacrine and ganglion neurons. That is, Ca^{2+} extrusion from photoreceptors and cone bipolar cells is mainly supported by PMCA1, whereas cell bodies of spiking retinal neurons possess PMCA3 and/or PMCA2 isoforms. Another isoform, PMCA4, apparently is localized to synaptic terminals of different classes of retinal neurons, as shown by colocalization with the synaptic marker SV2. This finding suggests that PMCA4 also participates in the regulation of synaptic transmission. Taken together, our results demonstrate that expression of Ca^{2+} pumps in retinal neurons is cell-type specific and suggest a functional link between the PMCA isoform type and neuronal function.

PMCA1 is localized to photoreceptors and cone bipolar cells

As opposed to the notion that PMCA1 is expressed by most, if not all, vertebrate cells (Stahl et al., 1992;Greb and Shull, 1989;Stauffer and Guerini, 1995;Stauffer et al., 1997), we found it to be expressed in a specific subset of retinal cells, that is, in photoreceptors, cone bipolar cells, and, possibly, horizontal cells. The expression of PMCA1 in photoreceptors was

confirmed by its colocalization with PSD-95 and SV2, two proteins commonly used as markers for photoreceptor terminals (e.g., Koulen et al., 1998;Vu et al., 2000). The selective localization of PMCA1 to photoreceptor terminals has been seen in all species we examined thus far (goldfish, salamander, rat, mouse, and monkey; unpublished observations). Our results further indicate that PMCA1 is not restricted to the synaptic "stalk" of photoreceptor terminals as recently seen in tree shrew cones with a pan-PMCA antibody (Morgans et al., 1998) nor is it localized exclusively to the active zone of the synapse as in the calyx-type presynaptic terminals of the chick ciliary ganglion (Juhaszova et al., 2000). In mouse photoreceptors, PMCA1 appears to be uniformly expressed throughout the synaptic terminals. Further electron microscopic studies will reveal whether PMCA1 is colocalized with voltage-gated Ca^{2+} channels at the arci-form densities immediately adjacent to the synaptic ribbons (Morgans et al., 1998;Nachman-Clewner et al., 1999) as well as with the glutamate receptors and transporters expressed at ectopic terminal sites (Eliasof et al., 1998;Fletcher et al., 2000). These results suggest that $[Ca^{2+}]_i$ at the sites of exocytosis in mouse photoreceptor terminals will be determined by highly localized cross-talk between Ca^{2+} influx and Ca^{2+} extrusion, rather than by a longitudinal Ca^{2+} gradient, as proposed by Morgans et al. (1998) for the tree shrew. Similar targeting of the PMCA1 isoform to the plasma membrane near synaptic release sites was reported recently for mammalian inner hair cells (Dumont et al., 2001). The colocalization of PMCA1 with PSD-95 additionally suggests that PDZ domain-containing proteins, which are abundantly expressed in photoreceptor terminals (Koulen et al., 1998;Vu et al., 2000) could act to organize PMCAs within presynaptic macromolecular complexes. Several splice variants of the PMCA family, including PMCA1b, contain the -ETSL/V C-terminal sequence, representing the consensus site for recognition of type I PDZ proteins, such as PSD-95 and SAP102 (DeMarco and Strehler, 2001). Therefore, if PMCA1 in photoreceptor terminals is tethered to PSD-95, we predict that these cells express splice variant 1b, similar to the synaptic membrane of inner hair cells (Dumont et al., 2001).

PMCA1 immunoreactivity in the mouse retina, however, was not confined to presynaptic sites of photoreceptors. Prominent PMCA1 signals also were observed in both IPL sublaminae. Moreover, weaker signals were noted in inner segments of photoreceptors and cell bodies of bipolar and horizontal cells. The expression of PMCA1 in synaptic terminals of bipolar cells was supported by the overlap of immunoreactivity between the PMCA1-immunostained IPL and the IPL labeled with an antibody against the vesicular glutamate transporter VGLUT1. Both VGLUT1 and PMCA1 stained similar populations of synaptic terminals in the IPL. Additional double-labeling experiments strongly suggested that PMCA1 is localized to the plasma membrane of cone, but not rod, bipolar cells. Rather, rod bipolar cell terminals expressed the PMCA2 isoform (see below). Our finding that Ca^{2+} extrusion from rod and cone bipolar cells is supported by different PMCA isoforms, complements a recent report showing that rod and cone bipolar cells possess different systems of Ca^{2+} regulation (Pan, 2000).

PMCA3 and PMCA2 are concentrated in the inner retina

Both PMCA2 and 3 antibodies label neurons situated in the GCL, IPL, and the inner edges of the INL. Although a weak PMCA2/PMCA3 signal is observed in the OPL at the level of horizontal cells, the staining pattern suggests that these two isoforms are likely to be used predominantly for Ca^{2+} clearance from retinal spiking neurons.

Electrophysiological recordings from GABAergic amacrine cells suggested variable contribution of PMCAs to clearance of Ca^{2+} across the plasma membranes of these cells (Gleason et al., 1994,1995). In these neurons, PMCAs cleared anywhere from 0 to ~50% of the total depolarization-evoked cytoplasmic Ca^{2+} load. The remaining percentage of Ca^{2+} was extruded by Na^+/Ca^{2+} exchange mechanisms, as observed in many other CNS neurons (Benham et al., 1992;Bindokas et al., 1994;Gleason et al., 1994,1995;Juhaszova et al., 2000).

The data of the present study indicate that, in addition to differences among subtypes of amacrine cells in the amount of the total PMCA protein (Gleason et al., 1995), amacrine cells also differ in expression of specific PMCA isoforms. For example, PMCA3 is found in some, but not all, GABAergic amacrine cells, whereas PMCA2 is much more widely expressed among these inhibitory interneurons. The perikarya and dendritic trees of amacrine cells may also contain different sets of PMCAs. Thus, in the INL, PMCA2 and PMCA3 were expressed by amacrine cell somata, whereas in the dense neuropil of the IPL, PMCA4 was found in addition to PMCA2 and PMCA3. We have not been able to determine whether different PMCA isoforms are colocalized within the same dendritic spines and presynaptic boutons. Electron microscopic analysis of amacrine/ganglion cell strata within the IPL will be required to settle this issue.

Functionally, PMCA2 and PMCA3 can be distinguished on the basis of their different affinities for Ca^{2+} and second messengers (Guerini, 1998;Guerini and Carafoli, 1998). PMCA2 has the highest affinity for calmodulin of all PMCA isoforms (Km ~5 nM; Elwess et al., 1997; Caride et al., 2001) and, thus, may be used for fine tuning of spatially restricted $[Ca^{2+}]_i$ changes at the level of amacrine and ganglion cell dendritic trees. Its "memory" for preceding Ca^{2+} spikes (Caride et al., 2001b) may invest it with an ability to regulate synaptic plasticity. Such a role for PMCA2 has been suggested for cerebellar Purkinje cells where PMCA2 is the major isoform in dendritic spines (Stauffer et al., 1997). In contrast, the affinity of PMCA3 for Ca^{2+} is lower compared with PMCA2 (Guerini, 1998), although some PMCA3 splice forms (e.g., 3f) show faster Ca^{2+} activation kinetics and are only minimally dependent on calmodulin activation (Caride et al., 2001a). PMCA3, thus, may contribute to Ca^{2+} clearance during large depolarizations. The importance of the PMCA2 pump for sensory function is underscored by the recent finding showing that PMCA2 gene "knockout" mice and mutant mice with a defective PMCA2 isoform possess selective deficits in auditory and vestibular function (Kozel et al., 1998;Street et al., 1998;Takahashi and Kitamura, 1999;Konrad-Martin et al., 2001). It remains to be seen whether similar defects in PMCA2 expression lead to dysfunctions during development of the mammalian retina and in synaptic transmission between retina and the brain.

Ca^{2+} extrusion mechanisms differ between cone and rod bipolar cells

A single rod bipolar cell type and at least nine subtypes of cone bipolar cells have been described in mammalian retinae. Cone bipolar cells include three to five distinct types of ON and three to five types of OFF bipolar neurons (Greferath et al., 1990;Euler and Wässle, 1995). Light depolarizes rod and ON cone bipolar cells and elevates free$[Ca^{2+}]_i$ in these cells by stimulating Ca^{2+} influx into the dendrites by means of mGluR6-gated conductances and by stimulating Ca^{2+} influx into cell bodies and synaptic terminals by means of voltage-gated Ca^{2+} channels (Protti and Llano, 1998;Shiells and Falk, 1999;Pan, 2000;Zenisek and Matthews, 2000). The ion channels that gate influx of Ca^{2+} into rod and cone bipolar cell terminals possess distinct physiological properties and may belong to different classes of channels (Protti and Llano, 1998;Pan, 2000). In this study, we present evidence that Ca^{2+} extrusion mechanisms also differ between rod and cone bipolar cells in at least two ways: (1) rod and cone bipolar cells express different PMCA isoforms, and (2) rod but not cone bipolar cells possess Na^+/Ca^{2+} exchangers. We found that PMCA1 was localized to cone bipolar cells, whereas PMCA2 was expressed in rod bipolar cells. Because the affinity of PMCA2 for calmodulin and Ca^{2+} is at least an order of magnitude higher compared with the affinity of most other PMCAs, Ca^{2+} extrusion from rod bipolar cells may be much more sensitive to small changes in $[Ca^{2+}]_i$ compared with that in cone bipolar cells. This sensitivity is consistent with the rod pathway being a high-gain pathway (Copenhagen et al., 1990). We also find, by using Ca^{2+} imaging, that a Na^+/Ca^{2+} exchange mechanism is prominently expressed in rod, but not cone, bipolar cells of the mouse retina. This report is the first physiological demonstration of

the important role of Na^+/Ca^{2+} exchange in clearing Ca^{2+} from mammalian bipolar cells. Our finding is consistent with a report by Kobayashi and Tachibana (1995) showing that Na^+/Ca^{2+} exchange contributes to clearance of large Ca^{2+} loads from the fish mixed Mb1 ON bipolar cell but differs from a recent report which suggested that Na^+/Ca^{2+} exchange plays little role in Ca^{2+} extrusion from synaptic terminals from Mb1 bipolar cells (Zenisek and Matthews, 2000). It is possible that the magnitude of intracellular Ca^{2+} loads in the latter study was not large enough to activate Na^+/Ca^{2+} exchange (e.g., Carafoli, 1991;Pozzan et al., 1994). Finally, our results are also consistent with functional data obtained by Ca^{2+} imaging from rat retinal slice preparations. Protti and Llano (1998) showed that there was no detectable rise in $[Ca^{2+}]_i$ in axons of rod bipolar cells during depolarization even when Ca^{2+} was imaged very close to synaptic terminals. These results are consistent with a highly effective mechanism, such as proposed for PMCA2, for removal of free Ca^{2+} in rod bipolar cells.

Physiological significance of differential localization of PMCA isoforms in the retina

The diversity of PMCA isoforms and their splice variants, together with their differential sensitivity for posttranslational modulation, suggests that different PMCA isoforms may be needed to selectively regulate Ca^{2+} homeostasis in different neurons or in different parts of the same cell (Dumont et al., 2001;Strehler and Zacharias, 2001). This hypothesis is further supported by our results, which show that PMCA isoforms are selectively localized to different classes of retinal neurons and, thus, are likely to play highly specific and selective roles in development, synaptic communication, and other processes requiring changes in $[Ca^{2+}]_i$. Subcellular targeting of PMCA isoforms has been reported for cochlear neurons. In these cells, PMCA2 is specifically targeted to hair cell stereocilia, whereas PMCA1 is localized to the basolateral membranes, suggesting specialized roles in mechanotransduction and synaptic function for PMCA2 and PMCA1, respectively (Dumont et al., 2001).

In darkness, depolarized photoreceptors and OFF bipolar cells are exposed to a sustained Ca^{2+} load by means of Ca^{2+} influx through voltage-gated Ca^{2+} channels located in cell bodies and synaptic terminals (Witkovsky et al., 1997;Protti and Llano, 1998). The conversion of the $[Ca^{2+}]_i$ signal into a rate of neurotransmitter release is characterized by an extreme sensitivity to changes in the membrane potential and $[Ca^{2+}]_i$ — photoreceptors can reliably transduce μV changes in the presynaptic voltage and nanomolar changes in $[Ca^{2+}]_i$ (Fain et al., 1977;Copenhagen et al., 1990;Rieke and Schwartz, 1996). PMCAs, with their high affinity for Ca^{2+} (Carafoli, 1991;Pozzan et al., 1994;Guerini, 1998) are well suited for regulating the magnitude and time course of the synaptic release at graded hyperpolarizing synapses. A crucial function of PMCA1 and PMCA4 may be to control the kinetics of the light response in cells postsynaptic to photoreceptors and OFF cone bipolar cells. The rate of the asynchronous transmitter release from photoreceptors and OFF bipolar cells should be determined principally by the kinetics of Ca^{2+} extrusion (e.g., Rieke and Schwartz, 1996). Factors modulating the activity of PMCA isoforms 1 and 4 (Carafoli, 1991;Guerini and Carafoli, 1998;Garcia and Strehler, 1999) should, therefore, regulate the time course of light responses from retinal cells.

However, uncontrolled high levels of Ca^{2+} in tonically depolarized neurons could also be associated with catabolic reactions leading to cell death, such as activation of phospholipases A and C, various proteases, disorganization of the cytoskeleton, and changes in nuclear chromatin (Edward et al., 1991;Trump and Berezesky, 1995). Part of the depolarization-evoked Ca^{2+} load in photoreceptors is probably neutralized by sequestration of Ca^{2+} into intracellular compartments (Krizaj et al., 1999). However, in the management of sustained Ca^{2+} loads that may occur in depolarized cells, a crucial role must be assigned to Ca^{2+} extrusion across the plasma membrane. PMCA1 and PMCA4 are the sole mechanism for Ca^{2+} extrusion from photoreceptor inner segments and synaptic terminals as well as in OFF cone bipolar cells.

Therefore, it is likely that these pumps are of key importance for the maintenance of normal photoreceptor cell function and signaling.

Amacrine and ganglion neurons are different from photoreceptors and bipolar cells in that they signal by means of bursts of Na^+-mediated and Ca^{2+}-mediated action potentials, which ride on top of a depolarizing plateau. These cells must, therefore, be able to cope with both large and transient changes in $[Ca^{2+}]_i$. Clearance of Ca^{2+} from amacrine cells occurs through synergistic action of Na^+/Ca^{2+} exchange mechanisms and PMCAs (Gleason et al., 1995). Na^+/Ca^{2+} exchangers are likely to be used for removal of large Ca^{2+} loads incurred by influx of Ca^{2+} through glutamate-gated and voltage-gated channels after prolonged depolarizations. During depolarizations, Na^+/Ca^{2+} exchangers may act in reverse (Levesque et al., 1991;Krizaj and Copenhagen, 1998;Micci and Christensen, 1998), and PMCAs (isoforms 2 and 3) may be needed to sustain Ca^{2+} homeostasis under these conditions. In addition, PMCAs may be needed to fine-tune changes in $[Ca^{2+}]_i$ and to maintain a low baseline $[Ca^{2+}]_i$ (Benham etal., 1992). The combined action of the two Ca^{2+} transporters is crucial for terminating transmitter release from these cells (Gleason et al., 1994). An interesting question that remains to be addressed in future work is whether the Ca^{2+} levels in retinal neurons may themselves be instrumental in the regulation of the transcription and expression of Ca^{2+} transporters. It has been shown recently that PMCA1, 2, and 3 are up-regulated by prolonged depolarization of neurons, whereas PMCA4 is down-regulated by high Ca^{2+} levels (Guerini et al., 1999). Similarly, up-regulation and down-regulation of various Na^+/Ca^{2+} exchanger isoforms was observed in high Ca^{2+} (Li et al., 2000). Thus, the pattern of neuronal steady-state $[Ca^{2+}]_i$ regulation may determine the most suitable set of Ca^{2+} pumps expressed.

In conclusion, our finding that PMCA1 is selectively expressed in photoreceptors and cone bipolar cells, that PMCA2 and PMCA3 are found in third-order neurons and that PMCA4 is expressed in synaptic terminals of retinal cells suggests that Ca^{2+} extrusion is highly regulated and functionally integrated with Ca^{2+} homeostasis in retinal cells. These conclusions raise several interesting questions concerning the precise role and regulation of different Ca^{2+} extrusion mechanisms during retinal cell function.

Acknowledgements

We thank Drs. Adelaida Filoteo and John T. Penniston (Mayo Clinic, Rochester, MN) for the generous gift of anti-PMCA antibodies and Mr. Michael C. Chicka for help with the immunoblots. We also thank Dr. Shigetada Nakanishi for the gift of the mGluR6 -/- and lacZ +/+ mice, Drs. René Renteria and Paul Witkovsky for comments on the manuscript, and Mr. Edwin Dumlao for technical assistance. D.R.C. and E.E.S. received funding from the National Institutes of Health, D.R.C. and D.K. received funding from the Wheeler Center for Neurobiology of Addiction, and D.R.C. is a recipient of an RPB Senior Investigator Award.

Grant sponsor: National Institutes of Health; Grant number: EY 01869; Grant number: EY02162; Grant number: NS16033; Grant sponsor: Wheeler Center for Neurobiology of Addiction.

LITERATURE CITED

Akopian A, Johnson J, Gabriel R, Brecha N, Witkovsky P. Somatostatin modulates voltage-gated K(+) and Ca(2+) currents in rod and cone photoreceptors of the salamander retina. J Neurosci 2000;20:929–936. [PubMed: 10648697]

Ausubel, FM.; Brent, R.; Kingston, RE.; Moore, DD.; Seidman, JG.; Smith, JA.; Struhl, K., editors. Current protocols in molecular biology. New York: John Wiley and Sons, New York; 1998.

Bellocchio EE, Hu H, Pohorille A, Chan J, Pickel VM, Edwards RH. The localization of the brain-specific inorganic phosphate transporter suggests a specific presynaptic role in glutamatergic transmission. J Neurosci 1998;18:8648–8659. [PubMed: 9786972]

Benham CD, Evans ML, McBain CJ. Ca^{2+} efflux mechanisms following depolarization evoked calcium transients in cultured rat sensory neurones. J Physiol 1992;455:567–583. [PubMed: 1484362]

Berridge MJ, Lipp P, Bootman MD. The versatility and universality of calcium signalling. Nat Rev Mol Cell Biol 2000;1:11–21. [PubMed: 11413485]

Bieda MC, Copenhagen DR. Sodium action potentials are not required for light-evoked release of GABA or glycine from retinal amacrine cells. J Neurophysiol 1999;81:3092–3095. [PubMed: 10368424]

Bindokas VP, Yoshikawa M, Ishida AT. Na^{+}-Ca^{2+} exchanger-like immunoreactivity and regulation of intracellular Ca^{2+} levels in fish retinal ganglion cells. J Neurophysiol 1994;72:47–55. [PubMed: 7965029]

Carafoli E. The calcium pumping ATPase of the plasma membrane. Annu Rev Physiol 1991;53:531–547. [PubMed: 1828335]

Caride AJ, Filoteo AG, Enyedi A, Verma AK, Penniston JT. Detection of isoform 4 of the plasma membrane calcium pump in human tissues by using isoform-specific monoclonal antibodies. Biochem J 1996;316:353–359. [PubMed: 8645230]

Caride AJ, Filoteo AG, Penheiter AR, Pàszty K, Enyedi À, Penniston JT. Delayed activation of the plasma membrane calcium pump by a sudden increase in Ca^{2+}: fast pumps reside in fast cells. Cell Calcium 2001a;30:49–57. [PubMed: 11396987]

Caride AJ, Penheiter AR, Filoteo AG, Bajzer Z, Enyedi A, Penniston JT. The plasma membrane calcium pump displays memory of past calcium spikes: differences between isoforms 2b and 4b. J Biol Chem 2001b;276:39797–39804. [PubMed: 11514555]

Copenhagen DR, Hemilä S, Reuter T. Signal transmission through the dark-adapted retina of the toad (Bufo marinus). Gain, convergence, and signal/noise. J Gen Physiol 1990;95:717–732. [PubMed: 2110968]

DeMarco SJ, Strehler EE. Plasma membrane Ca^{2+}-atpase isoforms 2b and 4b interact promiscuously and selectively with members of the membrane-associated guanylate kinase family of PDZ (PSD95/Dlg/ZO-1) domain-containing proteins. J Biol Chem 2001;276:21594–21600. [PubMed: 11274188]

de Talamoni N, Smith CA, Wasserman RH, Beltramino C, Fullmer CS, Penniston JT. Immunocytochemical localization of the plasma membrane calcium pump, calbindin-D28k, and parvalbumin in Purkinje cells of avian and mammalian cerebellum. Proc Natl Acad Sci U S A 1993;90:11949–11953. [PubMed: 8265654]

Dumont RA, Lins U, Filoteo AG, Penniston JT, Kachar B, Gillespie PG. Plasma membrane Ca^{2+}-ATPase isoform 2a is the PMCA of hair bundles. J Neurosci 2001;21:5066–5078. [PubMed: 11438582]

Eakin TJ, Antonelli MC, Malchiodi EL, Baskin DG, Stahl WL. Localization of the plasma membrane Ca(2+)-ATPase isoform PMCA3 in rat cerebellum, choroid plexus and hippocampus. Brain Res Mol Brain Res 1995;29:71–80. [PubMed: 7770003]

Edward DP, Lam TT, Shahinfar S, Li J, Tso MO. Amelioration of light-induced retinal degeneration by a calcium overload blocker. Flunarizine Arch Ophthalmol 1991;109:554–562.

Eliasof S, Arriza JL, Leighton BH, Kavanaugh MP, Amara SG. Excitatory amino acid transporters of the salamander retina: identification, localization, and function. J Neurosci 1998;18:698–712. [PubMed: 9425012]

Enyedi A, Verma AK, Heim R, Adamo HP, Filoteo AG, Strehler EE, Penniston JT. The Ca^{2+} affinity of the plasma membrane Ca^{2+} pump is controlled by alternative splicing. J Biol Chem 1994;269:41–43. [PubMed: 8276828]

Euler T, Wässle H. Immunocytochemical identification of cone bipolar cells in the rat retina. J Comp Neurol 1995;361:461–478. [PubMed: 8550893]

Fain GL, Granda AAM, Maxwell JH. Voltage signal of photoreceptors at the visual threshold. Nature 1977;265:181–183. [PubMed: 189205]

Famiglietti EV Jr, Kaneko A, Tachibana M. Neuronal architecture of on and off pathways to ganglion cells in carp retina. Science 1977;198:1267–1269. [PubMed: 73223]

Filoteo AG, Elwess NL, Enyedi A, Caride A, Aung HH, Penniston JT. Plasma membrane Ca^{2+} pump in rat brain. Patterns of alternative splices seen by isoform-specific antibodies. J Biol Chem 1997;272:23741–23747. [PubMed: 9295318]

Fletcher EL, Koulen P, Wässle H. $GABA_A$ and $GABA_C$ receptors on mammalian rod bipolar cells. J Comp Neurol 1998;396:351–365. [PubMed: 9624589]

Fletcher EL, Hack I, Brandstätter JH, Wässle H. Synaptic localization of NMDA receptor subunits in the rat retina. J Comp Neurol 2000;420:98–112. [PubMed: 10745222]

Garcia ML, Strehler EE. Plasma membrane calcium ATPases as critical regulators of calcium homeostasis during neuronal cell function. Front Biosci 1999;4:D869–D882. [PubMed: 10577388]

Gleason E, Borges S, Wilson M. Control of transmitter release from retinal amacrine cells by Ca^{2+} influx and efflux. Neuron 1994;13:1109–1117. [PubMed: 7524563]

Gleason E, Borges S, Wilson M. Electrogenic Na-Ca exchange clears Ca^{2+} loads from retinal amacrine cells in culture. J Neurosci 1995;15:3612–3621. [PubMed: 7751933]

Greb J, Shull GE. Molecular cloning of a third isoform of the calmodulin-sensitive plasma membrane Ca^{2+}-transporting ATPase that is expressed predominantly in brain and skeletal muscle. J Biol Chem 1989;264:18569–18576. [PubMed: 2530223]

Greferath U, Grünert U, Wässle H. Rod bipolar cells in the mammalian retina show protein kinase C-like immunoreactivity. J Comp Neurol 1990;301:433–442. [PubMed: 2262600]

Guerini D. The significance of the isoforms of plasma membrane calcium ATPase. Cell Tissue Res 1998;292:191–197. [PubMed: 9560462]

Guerini, D.; Carafoli, E. The calcium pumps. In: Carafoli, E.; Klee, C., editors. Calcium as a cellular regulator. New York: Oxford University Press; 1998.

Guerini D, Garcia-Martin E, Gerber A, Volbracht C, Leist M, Merino CG, Carafoli E. The expression of plasma membrane Ca^{2+} pump isoforms in cerebellar granule neurons is modulated by Ca^{2+} J Biol Chem 1999;274:1667–1676. [PubMed: 9880546]

Haverkamp S, Wässle H. Immunocytochemical analysis of the mouse retina. J Comp Neurol 2000;424:1–23. [PubMed: 10888735]

Hilfiker H, Guerini D, Carafoli E. Cloning and expression of isoform 2 of the human plasma membrane Ca^{2+} ATPase. Functional properties of the enzyme and its splicing products. J Biol Chem 1994;269:26178–26183. [PubMed: 7929331]

Johnson J, Caywood M, Reimer RJ, Edwards RH, Copenhagen DR. Vesicular neurotransmitter expression in developing postnatal rodent retina: GABA/glycine precedes glutamate. Soc Neurosci Abstr 2001;255:21a.

Juhaszova M, Church P, Blaustein MP, Stanley EF. Location of calcium transporters at presynaptic terminals. Eur J Neurosci 2000;12:839–846. [PubMed: 10762313]

Kobayashi K, Tachibana M. Ca^{2+} regulation in the presynaptic terminals of goldfish retinal bipolar cells. J Physiol 1995;483:79–94. [PubMed: 7539842]

Kolb H. Amacrine cells of the mammalian retina: neurocircuitry and functional roles. Eye 1995;11:904–923. [PubMed: 9537156]

Konrad-Martin D, Norton SJ, Mascher KE, Tempel BL. Effects of PMCA2 mutation on DPOAE amplitudes and latencies in deafwaddler mice. Hear Res 2001;151:205–220. [PubMed: 11124466]

Koulen P, Fletcher EL, Craven SE, Bredt DS, Wässle H. Immunocytochemical localization of the postsynaptic density protein PSD-95 in the mammalian retina. J Neurosci 1998;18:10136–10149. [PubMed: 9822767]

Kozel PJ, Friedman RA, Erway LC, Yamoah EN, Liu LH, Riddle T, Duffy JJ, Doetschman T, Miller ML, Cardell EL, Shull GE. Balance and hearing deficits in mice with a null mutation in the gene encoding plasma membrane Ca^{2+}-ATPase isoform 2. J Biol Chem 1998;273:18693–18696. [PubMed: 9668038]

Krizaj D, Copenhagen DR. Compartmentalization of calcium extrusion mechanisms in the outer and inner segments of photoreceptors. Neuron 1998;21:249–256. [PubMed: 9697868]

Krizaj D, Bao JX, Schmitz Y, Witkovsky P, Copenhagen DR. Caffeine-sensitive calcium stores regulate synaptic transmission from retinal rod photoreceptors. J Neurosci 1999;19:7249–7261. [PubMed: 10460231]

Levesque PC, Leblanc N, Hume JR. Role of reverse-mode Na(+)-Ca2+ exchange in excitation-contraction coupling in the heart. Ann N Y Acad Sci 1991;639:386–397. [PubMed: 1785865]

Li L, Guerini D, Carafoli E. Calcineurin controls the transcription of Na^{+}/Ca^{2+} exchanger isoforms in developing cerebellar neurons. J Biol Chem 2000;275:20903–20910. [PubMed: 10767288]

Masu M, Iwakabe H, Tagawa Y, Miyoshi T, Yamashita M, Fukuda Y, Sasaki H, Hiroi K, Nakamura Y, Shigemoto R, Takada M, Nakao K, Katsuki M, Nakanishi S. Specific deficit of the ON response in visual transmission by targeted disruption of the mGluR6 gene. Cell 1995;80:757–765. [PubMed: 7889569]

Micci MA, Christensen BN. Na^{+}/Ca^{2+} exchange in catfish retina horizontal cells: regulation of intracellular Ca^{2+} store function. Am J Physiol 1998;274:C1625–C1633. [PubMed: 9611128]

Miller JL, Picones A, Korenbrot JI. Differences in transduction between rod and cone photoreceptors: an exploration of the role of calcium homeostasis. Curr Opin Neurobiol 1994;4:488–495. [PubMed: 7812136]

Monteith GR, Roufogalis BD. The plasma membrane calcium pump: a physiological perspective on its regulation. Cell Calcium 1995;18:459–470. [PubMed: 8746945]

Morgans CW, El Far O, Berntson A, Wässle H, Taylor WR. Calcium extrusion from mammalian photoreceptor terminals. J Neurosci 1998;18:2467–2474. [PubMed: 9502807]

Nachman-Clewner M, St Jules R, Townes-Anderson E. L-type calcium channels in the photoreceptor ribbon synapse: localization and role in plasticity. J Comp Neurol 1999;415:1–16. [PubMed: 10540354]

Negishi K, Kato S, Teranishi T. Dopamine cells and rod bipolar cells contain protein kinase C-like immunoreactivity in some vertebrate retinas. Neurosci Lett 1988;94:247–252. [PubMed: 3205402]

Pan ZH. Differential expression of high- and two types of low-voltage-activated calcium currents in rod and cone bipolar cells of the rat retina. J Neurophysiol 2000;83:513–527. [PubMed: 10634892]

Pasteels B, Rogers J, Blachier F, Pochet R. Calbindin and calretinin localization in retina from different species. Vis Neurosci 1990;5:1–16. [PubMed: 2125465]

Penniston JT, Enyedi A. Modulation of the plasma membrane Ca^{2+} pump. J Membr Biol 1998;165:101–109. [PubMed: 9744998]

Pozzan T, Rizzuto R, Volpe P, Meldolesi J. Molecular and cellular physiology of intracellular calcium stores. Physiol Rev 1994;74:595–636. [PubMed: 8036248]

Protti DA, Llano I. Calcium currents and calcium signaling in rod bipolar cells of rat retinal slices. J Neurosci 1998;18:3715–3724. [PubMed: 9570802]

Rieke F, Schwartz EA. Asynchronous transmitter release: control of exocytosis and endocytosis at the salamander rod synapse. J Physiol 1996;493:1–8. [PubMed: 8735690]

Shiells RA, Falk G. A rise in intracellular Ca^{2+} underlies light adaptation in dogfish retinal “on” bipolar cells. J Physiol 1999;514:343–350. [PubMed: 9852318]

Stahl WL, Eakin TJ, Owens JW Jr, Breininger JF, Filuk PE, Anderson WR. Plasma membrane Ca(2+)-ATPase isoforms: distribution of mRNAs in rat brain by in situ hybridization. Brain Res Mol Brain Res 1992;16:223–231. [PubMed: 1337931]

Stauffer T, Guerini D. Tissue distribution of the four gene products of the plasma membrane Ca^{2+} pump. J Biol Chem 1995;270:12184–12190. [PubMed: 7538133]

Stauffer T, Guerini D, Celio MR, Carafoli E. Immunolocalization of the plasma membrane Ca^{2+} pump isoforms in the rat brain. Brain Res 1997;748:21–29. [PubMed: 9067441]

Street VA, McKee-Johnson JW, Fonseca RC, Tempel BL, Noben-Trauth K. Mutations in a plasma membrane Ca^{2+}-ATPase gene cause deafness in deafwaddler mice. Nat Genet 1998;19:390–394. [PubMed: 9697703]

Strehler EE, Zacharias DA. Role of alternative splicing in generating isoform diversity among plasma membrane calcium pumps. Physiol Rev 2001;81:21–50. [PubMed: 11152753]

Szel A, Rohlich P, Caffe AR, van Veen T. Distribution of cone photoreceptors in the mammalian retina. Microsc Res Tech 1996;35:445–462. [PubMed: 9016448]

Takahashi K, Kitamura K. A point mutation in a plasma membrane Ca^{2+}-ATPase gene causes deafness in Wriggle Mouse Sagami. Biochem Biophys Res Commun 1999;261:773–778. [PubMed: 10441500]

Trump BF, Berezesky IK. Calcium-mediated cell injury and death. FASEB J 1995;220:219–228. [PubMed: 7781924]

Ueda Y, Iwakabe H, Masu M, Suzuki M, Nakanishi S. The mGluR6 5’ upstream transgene sequence directs a cell-specific and developmentally regulated expression in retinal rod and ON-type cone bipolar cells. J Neurosci 1997;17:3014–3023. [PubMed: 9096137]

Usachev YM, Toutenhoofd SL, Goellner GM, Strehler EE, Thayer SA. Differentiation induces up-regulation of plasma membrane Ca^{2+}-ATPase and concomitant increase in Ca^{2+} efflux in human neuroblastoma cell line IMR-32. J Neurochem 2001;76:1756–1765. [PubMed: 11259493]

Vu TQ, Payne JA, Copenhagen DR. Localization and developmental expression patterns of the neuronal K-Cl cotransporter (KCC2) in the rat retina. J Neurosci 2000;20:1414–1423. [PubMed: 10662832]

Werblin FS, Dowling JE. Organization of the retina of the mudpuppy, Necturus maculosus. II. Intracellular recording. J Neurophysiol 1969;32:339–355. [PubMed: 4306897]

Witkovsky P, Schmitz Y, Akopian A, Krizaj D, Tranchina D. Gain of rod to horizontal cell synaptic transfer: relation to glutamate release and a dihydropyridine-sensitive calcium current. J Neurosci 1997;17:7297–7306. [PubMed: 9295376]

Zenisek D, Matthews G. The role of mitochondria in presynaptic calcium handling at a ribbon synapse. Neuron 2000;25:229–237. [PubMed: 10707986]

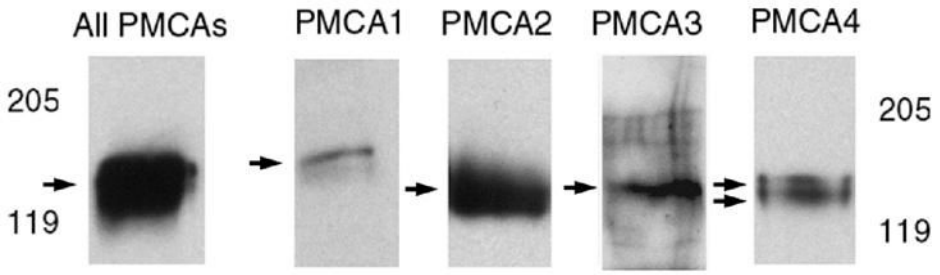

Fig 1.

Western blot analysis shows plasma membrane calcium ATPase (PMCA) isoform expression in the adult mouse retina. Total protein lysates (40 μg protein per lane) from adult mouse retinae were separated on 7.5% sodium dodecyl sulfate-polyacrylamide gels, blotted onto polyvinylidene difluoride membrane, and processed for Western blotting by using PMCA isoform-specific antibodies NR1 (PMCA1), NR2 (PMCA2), NR3 (PMCA3), and NR4/JA9 (PMCA4). The pan-PMCA antibody 5F10 was used as a control to detect the sum of all PMCAs (All PMCAs). Molecular mass standards are indicated in kilodaltons on the sides, and the bands are marked by arrows.

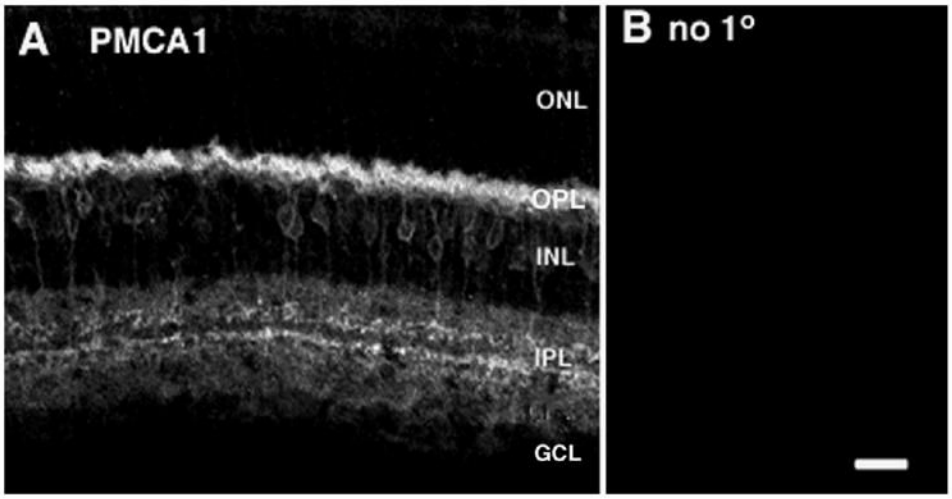

Fig 2.

Confocal fluorescence photomicrograph of a vertical frozen section through mouse retina labeled for plasma membrane calcium ATPase (PMCA)1plus secondary antibody (**A**) or with the secondary antibody only (**B**). A: PMCA1 immunofluorescence is prominent in the outer plexiform layer (OPL). Moderate PMCA1 signal is also observed in bipolar cell perikarya in the upper part of the inner nuclear layer (INL) and in the inner plexiform layer (IPL). ONL, outer nuclear layer; GCL, ganglion cell layer. Scale bar = 20 μm in B (applies to A,B).

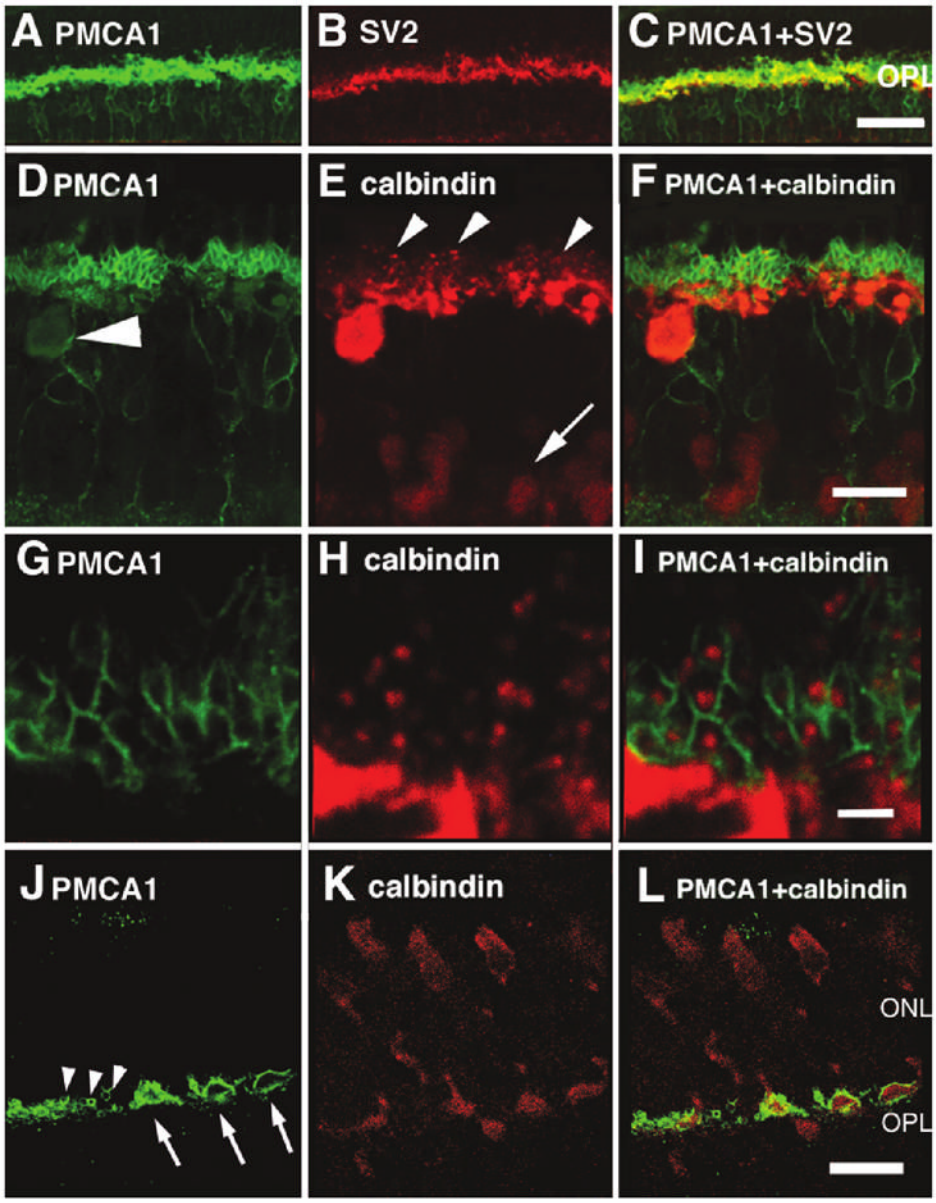

Fig 3.

Confocal fluorescence labeling indicates plasma membrane calcium ATPase 1 (PMCA1) expression in photoreceptor terminals. **A:** PMCA1 is strongly expressed in the outer plexiform layer (OPL), where it labels a horizontal band of ellipsoid structures corresponding to photoreceptor terminals. Moderate label is also present in perikarya of bipolar cells in the inner nuclear layer (INL). **B:** SV2 immunolabels photoreceptor synaptic terminals. **C:** Superposition of PMCA1 and SV2 immunofluorescence indicates substantial colocalization between the two antibodies in photoreceptor terminals. D–I: Higher power confocal fluorescence photomicrographs of immunoreactivity for PMCA1 and calbindin show colabeling of horizontal cells but not of photoreceptors, amacrine, or ganglion cells. **D:** PMCA1 is prominently expressed in photoreceptor synaptic terminals. The labeling is moderate in bipolar cell bodies in the distal INL and weak in horizontal cells (arrowhead). **E:** Calbindin antibody strongly labels horizontal cells. Prominent somas with dendritic knobs, extending into photoreceptor terminals (arrowheads), are observed. The antibody also labels a population of

amacrine cells located in the proximal INL (arrow). **F:** Superposition of images from D and E. PMCA1 is expressed in photoreceptor terminals but is excluded from calbindin-immunopositive amacrine cells. **G–I:** High-power fluorescence photomicrograph of the same section as shown in D–F with magnification focused on the OPL. Each dendritic knob emanating from horizontal cells is associated with exactly one photoreceptor terminal immunolabeled by PMCA1. J–L: Section through macaque monkey retina immunostained for PMCA1 and calbindin. **J:** PMCA1 immunostained the two types of synaptic terminals in the OPL. Note that synaptic terminals are labeled uniformly. **K:** Calbindin selectively stains a population of monkey cones. **L:** PMCA1 signal is expressed in rod spherules (arrowheads) as well as in cone pedicles (arrows). Scale bars = 15 μm in C (applies to A–C), 10 μm in F (applies to D–F), 2.5 μm in I (applies to G–I), 20 μm in L (applies to J–L).

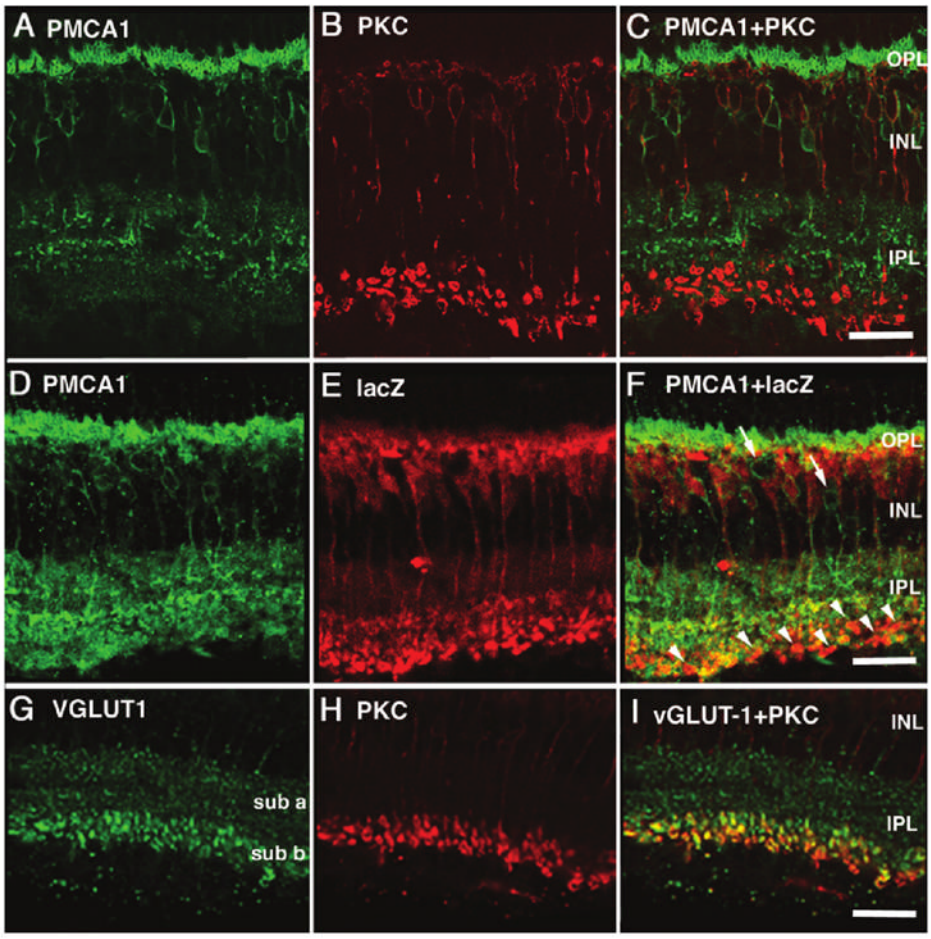

Fig 4.

Plasma membrane calcium ATPase 1 (PMCA1) is expressed in cone but not rod bipolar cells. A–C: Double labeling for PMCA1 (**A**) and protein kinase C (PKC; **B**). PKC immunolabeled dendritic trees, perikarya, and synaptic terminals of rod bipolar cells. **C:** Little colocalization is observed between the PMCA1-immunopositive cells and PKC-immunopositive rod bipolar cells. D–F: Double labeling for β-galactosidase in the lacZ transgenic mouse. **D:** PMCA1 signal in the lacZ mutant is higher than in the wild-type control (Fig. 4A). **E:** β-Galactosidase antibody immunolabels a large population of cells with synaptic terminals in sublamina b of the inner plexiform layer (IPL). **F:** Significant colocalization is observed between PMCA1 and lacZ immunopositive perikarya in the INL. The lacZ-immunopositive terminals in the proximal IPL were typically unlabeled by PMCA1 (arrowheads). G–I: Double-labeling for vesicular glutamate transporter (VGLUT1) and PKC. **G:** VGLUT1 is expressed in glutamatergic synaptic terminals localized to both sublamina a (sub a) and sublamina b (sub b) of the IPL. **H:** Labeling for PKC. **I:** Colocalization of VGLUT1 and PKC signals in terminals of rod bipolar cells. The PMCA1-immunopositive puncta in sublamina b, unlabeled by the PKC antibody, correspond to synaptic terminals of ON cone bipolar cells. The PMCA1-immunopositive puncta in sub-lamina a, unlabeled by the PKC antibody, correspond to OFF cone bipolar cells terminals. Scale bars = 20 μm in C (applies to A–C) and I (applies to G–I), 25 μm in F (applies to D–F).

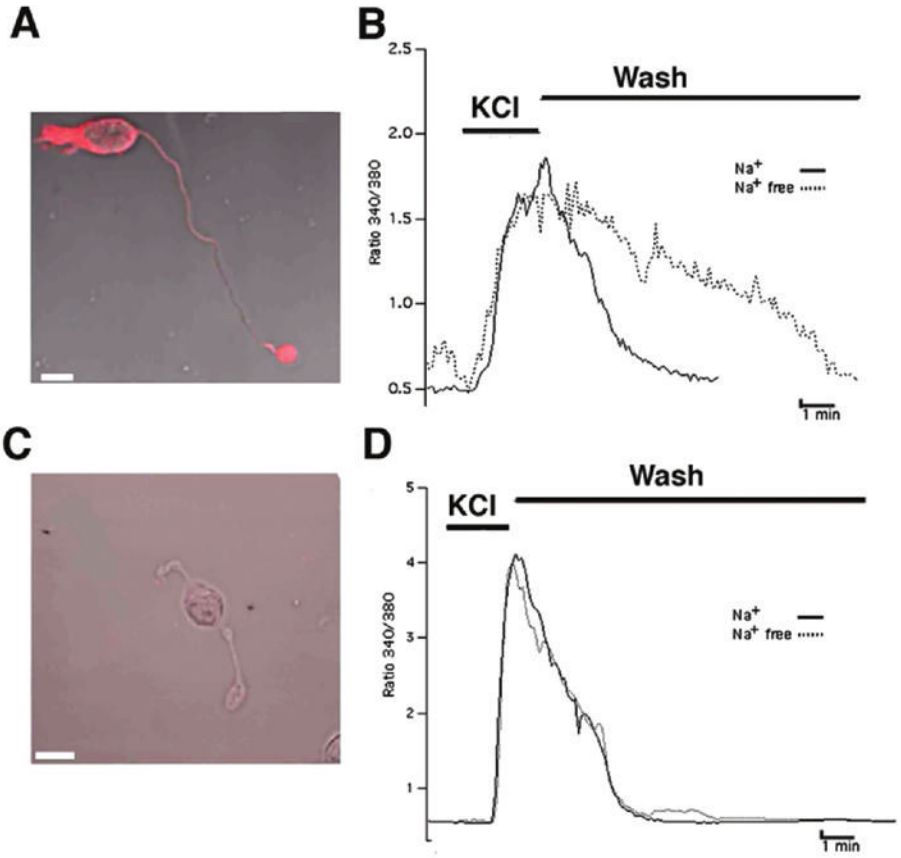

Fig 5.

Ca^{2+} extrusion from rod and cone bipolar cells. **A:** Combined Nomarski and fluorescence photomicrograph of a rod bipolar cell dissociated from the mouse retina and immunostained for protein kinase C (PKC). The antibody labeled the cell body, the axon, and the synaptic terminal. **B:** $[Ca^{2+}]_i$ changes in a fura-2 loaded rod bipolar cell are shown as changes in the ratio between 340- and 380-nm wavelengths. The cell was superfused with 45 mM KCl (horizontal bar labeled KCl). At t = 2.3 min, the solution was switched (horizontal line labeled Wash) to a control 2.5 mM K^+ -containing saline (solid line) or a test 2.5 mM K^+ saline in which $[Na^+]_o$ was substituted by $[Li^+]_o$ (dotted line). $[Ca^{2+}]_i$ recovery to the baseline value after a depolarization-evoked increase in significantly prolonged in the absence of $[Na^+]_o$ **C:** A small proportion of bipolar cells were not labeled by the PKC antibody. These cells were classified as putative cone dipolar cells. **D:** $[Ca^{2+}]_i$ changes in a fura-2 loaded putative cone bipolar cell are shown as changes in the ratio between 340- and 380-nm wavelengths. The cell was depolarized (horizontal bar labeled KCl) with 45 mM KCl and then superfused (horizontal bar labeled Wash) with control saline (solid line) or a test saline in which $[Na^+]_o$ was substituted by $[Li^+]_o$ (dotted line). During washout with control saline, $[Ca^{2+}]_i$ recovered to the baseline value exponentially with two time constants that were very similar in control and Li^+ saline. Scale bars = 5 μm in A, 5 μm in C.

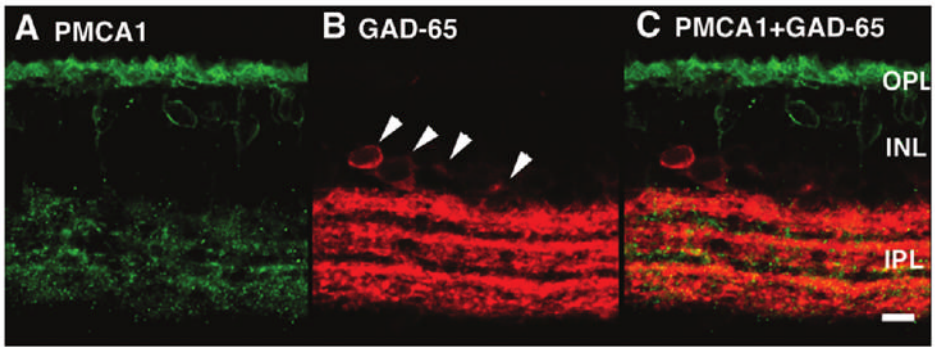

Fig 6.

Plasma membrane calcium ATPase 1 (PMCA1) is not localized to γ-aminobutyric acid-ergic neurons. Sections were labeled for PMCA1 and glutamic acid decarboxylase 65 (GAD-65). **A:** PMCA1 labeled the outer plexiform layer (OPL), inner plexiform layer (IPL), and the inner nuclear layer (INL). **B:** The same section as in A immunolabeled for GAD-65. The label is restricted to amacrine cell bodies in the INL (arrowheads) and to amacrine processes in the IPL. **C:** Superposition of A and B shows little apparent colocalization of PMCA1 and GAD-65 in the INL. Scale bar = 10 μm in C (applies to A–C).

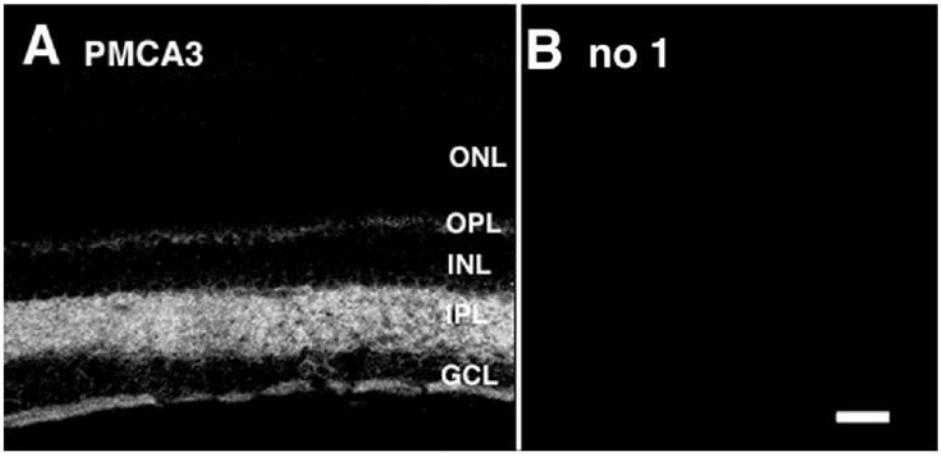

Fig 7.

Plasma membrane calcium ATPase 3 (PMCA3) immunoreactivity in the mouse retina. **A:** The PMCA3 immunofluorescence is prominent throughout the inner plexiform layer (IPL). Amacrine cell bodies in the inner nuclear layer (INL) and ganglion cell bodies in the granule cell layer (GCL) are also labeled. The optic nerve fiber layer is strongly labeled. Weaker immunofluorescence is observed in the outer plexiform layer (OPL). ONL, outer nuclear layer. **B:** Section stained with secondary antibody only. Scale bar = 20 μm.

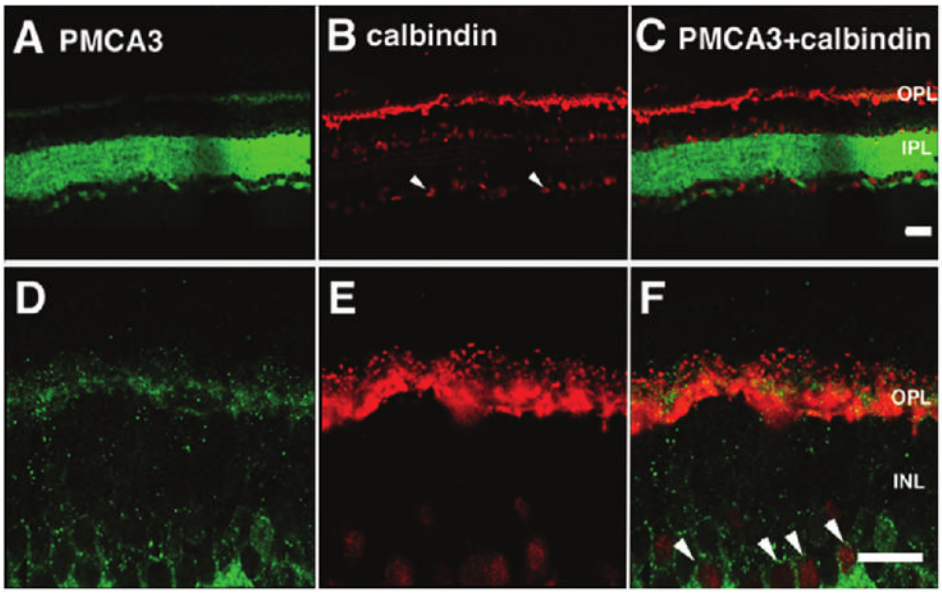

Fig 8.

Plasma membrane calcium ATPase 3 (PMCA3) and calbindin immunoreactivity demonstrate expression of PMCA3 in horizontal and amacrine cells. **A:** Section labeled for PMCA3. **B:** Same section shown in A labeled for calbindin. **C:** Horizontal cells, amacrine cells and displaced amacrine cells (arrowheads) are immunoreactive for both PMCA3 and calbindin. D–F. Same section as in A–C at higher magnification. OPL, outer plexiform layer; IPL, inner plexiform layer. **D:** PMCA3 is localized to horizontal cell bodies and processes and to amacrine cell bodies lining the proximal inner nuclear layer (INL). **E:** Same section as in D labeled for calbindin. **F:** Double-labeling for PMCA3 and calbindin. Both antigens are expressed in horizontal cells and in amacrine cells (arrowheads). Scale bar = 20 μm in C (applies to A–C), 15 μm in F (applies to A–F).

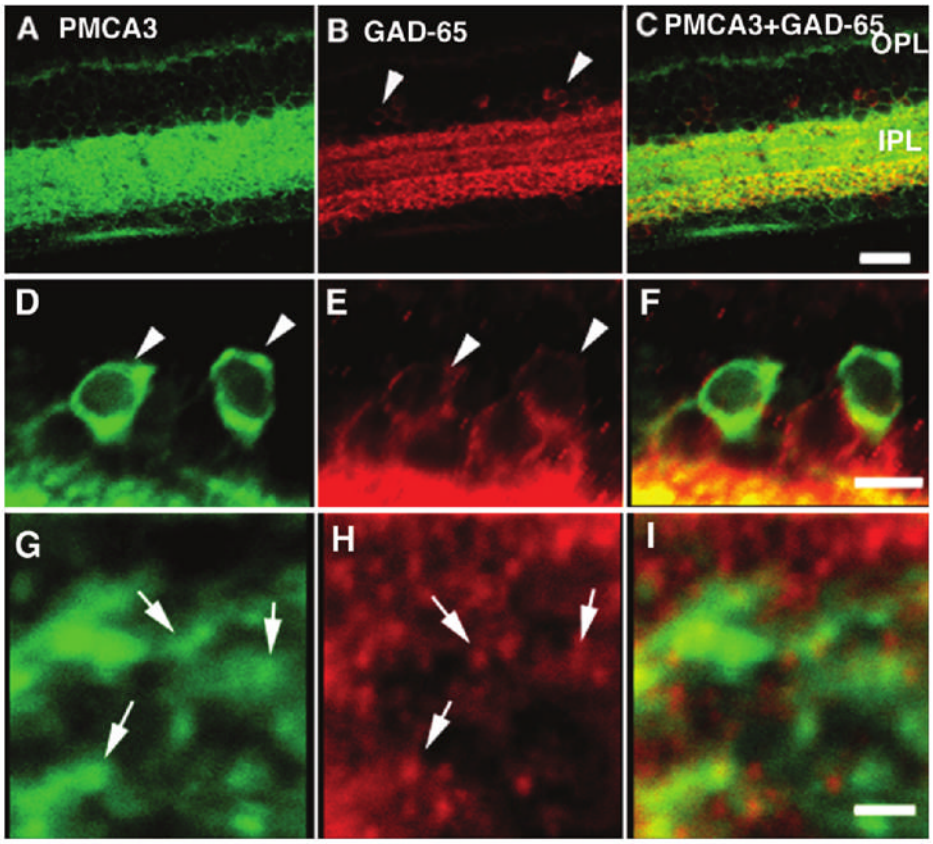

Fig 9.

Colocalization of plasma membrane calcium ATPase 3 (PMCA3) and glutamic acid decarboxylase 65 (GAD-65) expression. **A:** PMCA3 immunoreactivity is expressed in both plexiform layers (inner, IPL; outer, OPL), the inner nuclear layer (INL), and the granule cell layer. **B:** Same section shown in A labeled for GAD-65. GAD-65 immunofluorescence is found in perikarya of amacrine cells localized to the proximal INL (arrowheads). Prominent immunoreactivity can be seen in the IPL. **C:** PMCA3 and GAD-65 colocalize in amacrine cell bodies in the INL. D–I: Same section shown at high magnification for INL (D–F) and IPL (G–I) labeled for PMCA3 (D and G) and GAD-65 (E,F). **D:** PMCA3 is expressed in a subset of perikarya at the proximal edge of the INL. **E:** GAD-65 labels perikarya in the proximal INL. **F:** PMCA3 is colocalized with GAD-65 in a subset of GAD-65–immunoreactive neurons in the INL (arrowheads in D,E). **G:** High-power photomicrograph of a PMCA3-immunolabeled retina focused on the IPL. PMCA3 antibody labeled distinct puncta within the IPL (arrows). **H:** Same section as in G labeled for GAD-65. GAD-65 immunolabeled distinct puncta in the IPL (arrows). **I:** PMCA3 and GAD-65 immunofluorescence colocalized in many puncta (arrows in G and H). Scale bars = 20 μm in C (applies to A–C), 7.5 μm in F (applies to D–F), 1.5 μm in I (applies to G–I).

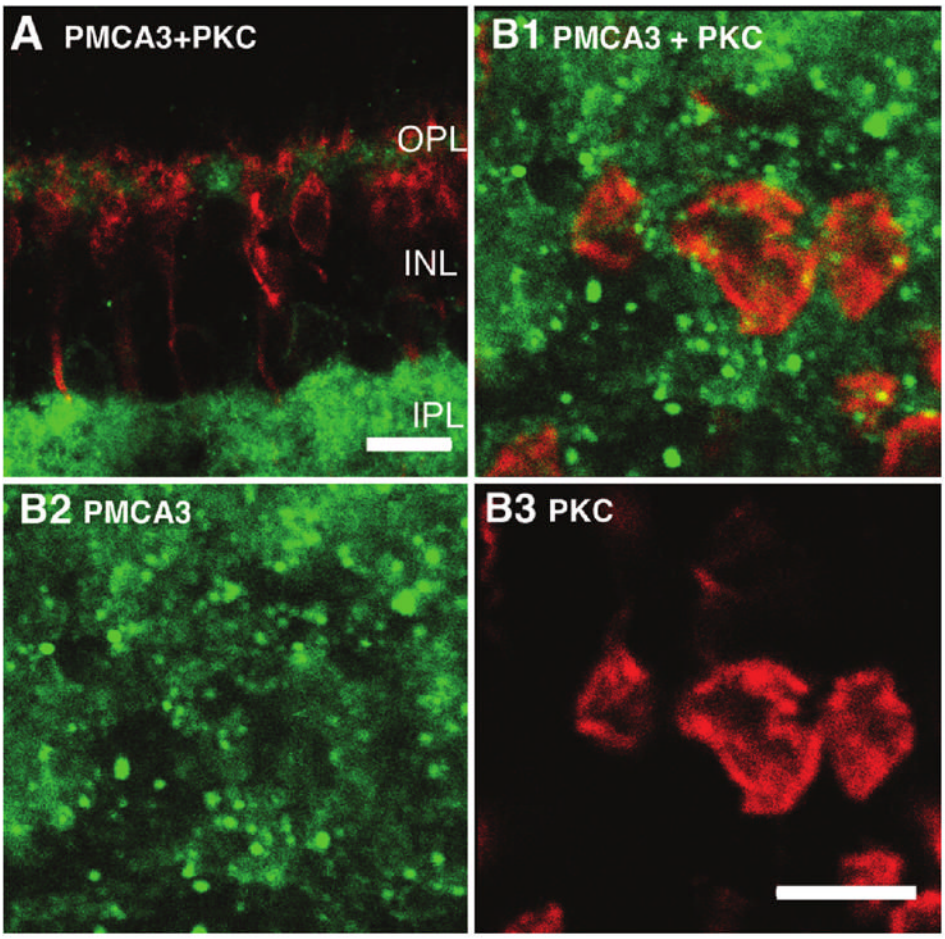

Fig 10.

Plasma membrane calcium ATPase 3 (PMCA3) is not expressed in rod bipolar cell bodies and synaptic terminals. **A:** Outer plexiform layer (OPL) and inner nuclear layer (INL) regions double labeled for PMCA3 (green) and protein kinase C (PKC; red). PMCA3 is not expressed in perikarya of rod bipolar cells. B1–3: Same section, magnified view of the IPL. **B1:** Little colocalization between PMCA3 and PKC is seen at the level of rod bipolar cell terminals. **B2:** Same section as B1; PMCA3 signal in the IPL. **B3:** Same section as B1; PKC in the IPL immunolabels synaptic terminals of rod bipolar cells. Scale bars = 10 μm in A; 7.5 μm in B3 (applies to B1–3).

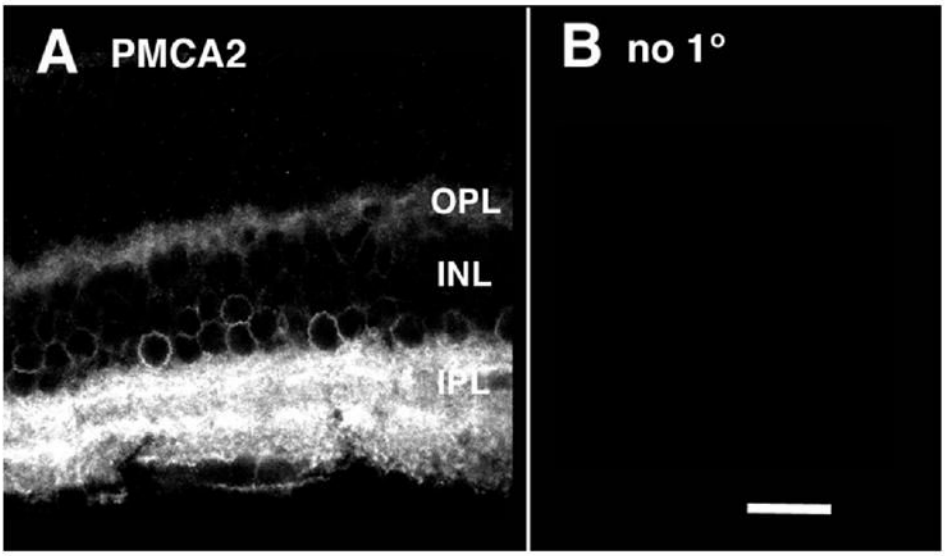

Fig 11.

Plasma membrane calcium ATPase 2 (PMCA2) immunolocalization in the mouse retina. **A:** The PMCA2 antibody labeled the IPL with the most prominent signal shown in two strata in sublaminae a and b, respectively. Moderate immunoreactivity is seen in the outer plexiform layer (OPL) and in the proximal inner nuclear layer (INL). **B:** Section stained with secondary antibody only. Scale bar = 20 μm in B (applies to A,B).

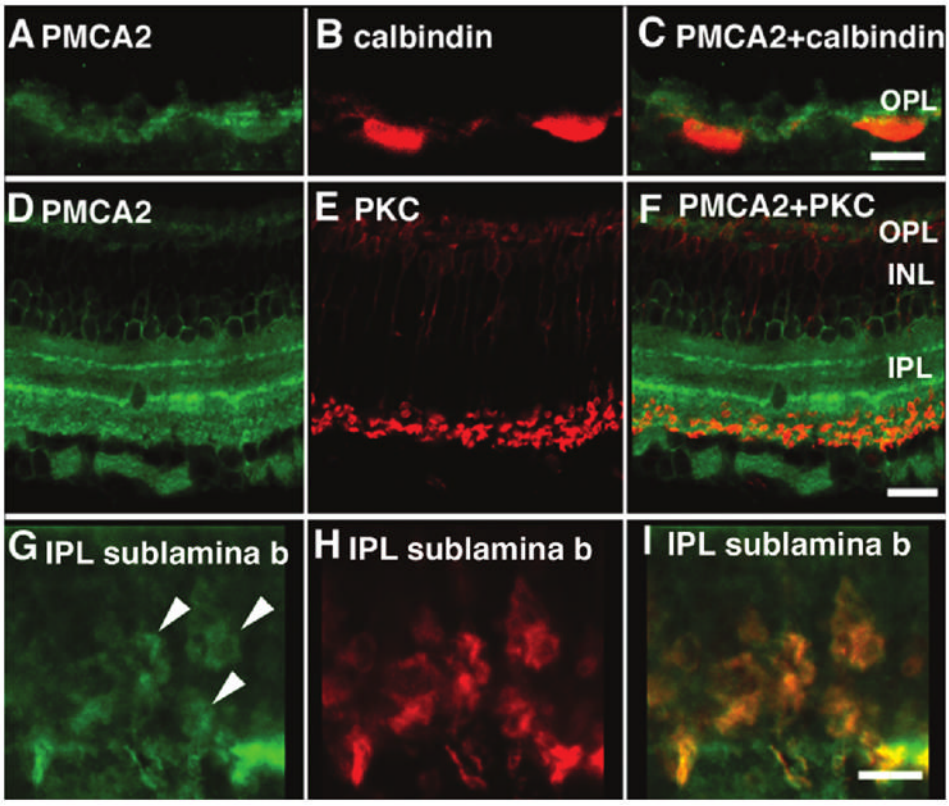

Fig 12.

Plasma membrane calcium ATPase 2 (PMCA2) is expressed in synaptic terminals of rod bipolar cells and in horizontal cells. **A:** Magnified view of the outer plexiform layer (OPL) labeled for PMCA2. PMCA2 is expressed diffusively throughout the OPL. **B:** Same section immunolabeled for calbindin. Calbindin immunofluorescence is found in horizontal cells. **C:** PMCA2 and calbindin colocalize in horizontal cell bodies and dendrites. D–F: Retinal section double labeled for PMCA2 and protein kinase C (PKC). **D:** PMCA2 signal in a low-power photomicrograph. **E:** Same section showing the PKC signal. **F:** Double labeling for PMCA2 and PKC. INL, inner nuclear layer. G–I. Same section as in D–F, high-power view focused on sublamina b of the inner plexiform layer (IPL). **G:** PMCA2 immu-noreactivity in sublamina b. **H:** PKC immunoreactivity in sublamina b. **I:** Colocalization with PMCA2 is seen in synaptic terminals of PKC-immunoreactive rod bipolar cell synaptic terminals (arrowheads in G). Scale bars = 10 μm in C (applies to A–C), 20 μm in F (applies to D–F), 8 μm in I (applies to G–I).

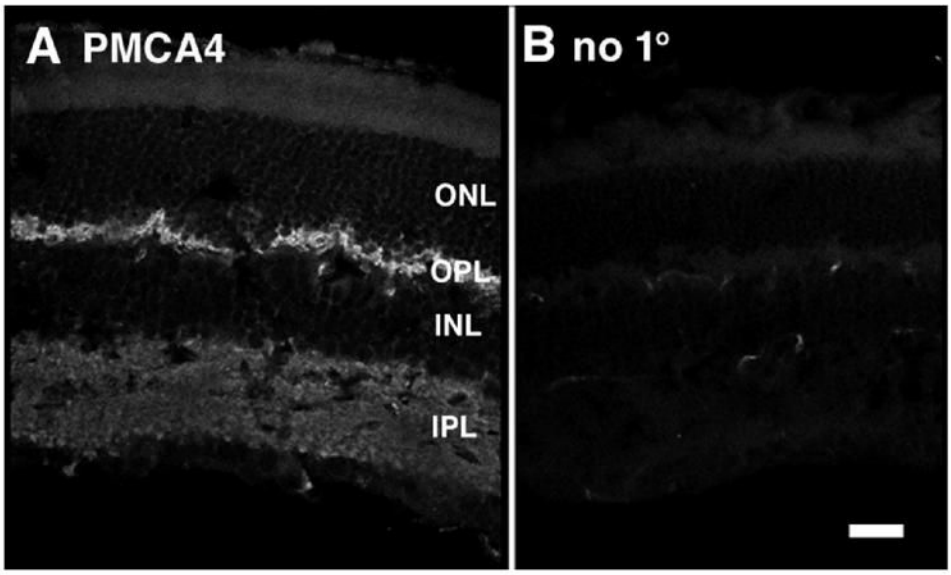

Fig 13.

Plasma membrane calcium ATPase 4 (PMCA4) immunolocalization in the retina. **A:** PMCA4 immunostained both plexiform layers (outer, OPL; inner, IPL). Nonspecific signal is seen at the level of photoreceptor outer segments. INL, inner nuclear layer; ONL, outer nuclear layer. **B:** Section stained with secondary antibody only. Scale bar = 20 μm.

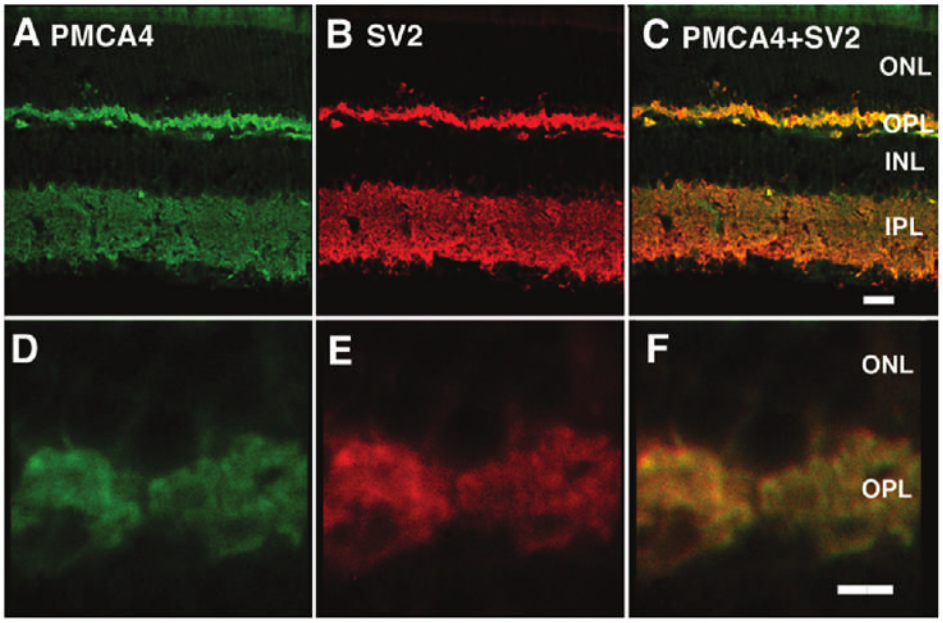

Fig 14.

Plasma membrane calcium ATPase 4 (PMCA4) is localized to synaptic terminals. **A:** PMCA4 is prominently expressed in the outer plexiform layer (OPL) and the inner plexiform layer (IPL). **B:** Same section labeled for SV2. **C:** Combined images for the section shown in A and B show high degree of colocalization in both synaptic layers for PMCA4 and SV2 signals. ONL, outer nuclear layer; INL, inner nuclear layer. **D–F:** Higher magnification view of the section shown in A–C, focusing on the OPL. Note the colocalization of PMCA4 and SV2 in photoreceptor terminals. Scale bar = 20 μm in C (applies to A–C), 2 μm in F (applies to D–F).

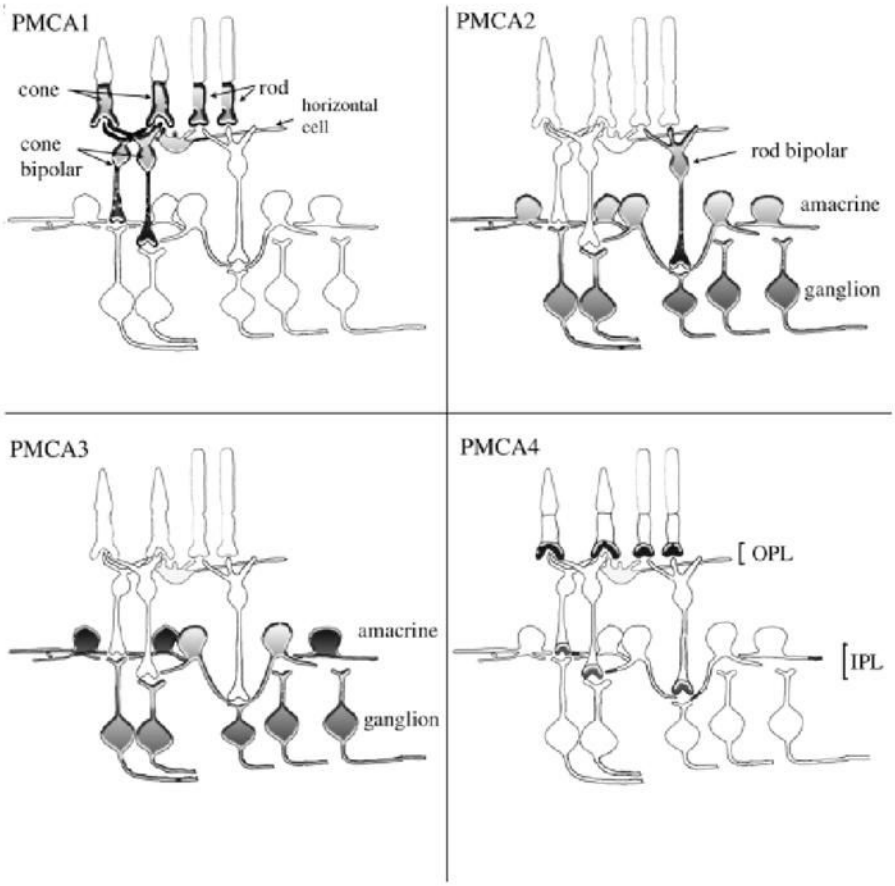

Fig 15.

Schematic localization of plasma membrane calcium AT-Pase (PMCA) isoforms in the mammalian retina. The distribution of PMCA isoforms is indicated by shading of neuronal classes associated with the appropriate isoform. PMCA was expressed in photoreceptors and cone bipolar cells. Weak signal was also observed in horizontal cells. PMCA2 was present in rod bipolar cells, amacrine cells, and ganglion cells. PMCA3 was highly expressed in amacrine and ganglion cells, and weakly in horizontal cells. PMCA4 was found to label synaptic elements in the outer plexiform layer (OPL) at the level of photoreceptor terminals, and in the inner plexiform layer (IPL) where synaptic terminals of bipolar and amacrine cells are found.